# Thermomechanical Constitutive Models of Shape Memory Polymers and Their Composites

**5 authors**, including:

Wei Zhao
Harbin Institute of Technology
**30** PUBLICATIONS **576** CITATIONS

SEE PROFILE

Xin Zhe Lan
Shaanxi open university
**98** PUBLICATIONS **3,637** CITATIONS

SEE PROFILE

Yanju Liu
Harbin Institute of Technology
**317** PUBLICATIONS **11,102** CITATIONS

SEE PROFILE

**Some of the authors of this publication are also working on these related projects:**

Mechanical behavior characterization View project

Aerospace design View project

## Wei Zhao
Department of Astronautical Science and
Mechanics,
Harbin Institute of Technology (HIT),
No. 92 West Dazhi Street,
P.O. Box 301,
Harbin 150001, China

## Liwu Liu
Department of Astronautical Science and
Mechanics,
Harbin Institute of Technology (HIT),
No. 92 West Dazhi Street,
P.O. Box 301,
Harbin 150001, China

## Xin Lan
Centre for Composite Materials,
Harbin Institute of Technology (HIT),
No. 2 YiKuang Street,
P.O. Box 3011,
Harbin 150080, China

## Jinsong Leng[1]
Centre for Composite Materials,
Harbin Institute of Technology (HIT),
No. 2 YiKuang Street,
P.O. Box 3011,
Harbin 150080, China
e-mail: lengjs@hit.edu.cn

## Yanju Liu[1]
Department of Astronautical Science and
Mechanics,
Harbin Institute of Technology (HIT),
No. 92 West Dazhi Street,
P.O. Box 301,
Harbin 150001, China
e-mail: yj_liu@hit.edu.cn

# Thermomechanical Constitutive Models of Shape Memory Polymers and Their Composites

*Shape memory polymers (SMPs) and SMP composites (SMPCs) have been widely employed in several fields and exhibit excellent self-actuation, deformation, and self-adaption. Establishing reasonable constitutive models is vital for understanding the shape memory mechanism and expanding its applications. Moreover, the mechanical response of SMPs under different conditions can be predicted, facilitating their precise control. The internal mechanism for the shape memory behavior in most SMPs is thermal actuation. This study reviews the theories of thermally actuated SMPs, rheological and phase transition concept models, and models combining the rheology and phase transition concepts. Furthermore, the constitutive models of particulate-reinforced SMPCs, carbon-fiber-reinforced SMPCs, and the buckling behavior of SMPCs are summarized. This study is expected to help solve the remaining issues rapidly and contribute to the establishment of rational constitutive models for SMPs and SMPCs.*
[DOI: 10.1115/1.4056131]

*Keywords: shape memory, constitutive model, thermomechanical, rheology, phase transition*

## 1 Introduction

As a class of stimulus-responsive materials, shape memory polymers (SMPs) can switch between programed and permanent states under appropriate external stimuli [1–6]. Shape memory effect (SME) refers to the storage and recovery of deformation under corresponding environmental stimulations [7]. The SME can be actuated using various actuation methods; however, for most of these methods, heat is the main actuator. The temperature transition between the fixed phase, dominated by entropy, and the reversible phase, dominated by internal energy, provides a basic thermodynamic interpretation for the SME.

The trigger mechanisms of SME depend on the polymer system. SMPs with physical crosslinking are typically called thermoplastic SMPs and are comprised of physically entangled and crystallized molecular chains. For this type of SMP, the SME is caused by the interaction between the hard and soft segments of the macromolecule in the internal structure. When an external load is applied, the hard chain segment is responsible for transporting and transferring the load. Under the stimulation of an external load, the hard chain segment gradually transforms into a soft chain segment. The soft chain segment is responsible for storing the deformation and releasing it under certain conditions to achieve shape recovery.

Molecular chains in thermosetting SMP are entangled with each other by chemical crosslinking, which primarily occurs as covalent bonding between the macromolecular chains. For this type of SMP, the fluidity of the molecular chain varies exponentially owing to variations in temperature during the glass transition process, and the macroscopic manifestation is the SME. With an increase in temperature, the fluidity of the molecular chains gradually increases. The SMP reacts rapidly to the external load, and the molecular network moves toward the decreasing configuration entropy. However, with a decrease in temperature, the fluidity of the molecular chain weakens gradually, resulting in a delayed reaction to the external load. When the temperature drops below the glass transition temperature ($T_g$), the fluidity of the molecular chains gradually reaches their freezing point, and achieving the equilibrium state under external load is difficult. At the macroscopic level, the cooling process increases the stiffness of the SMP, resulting in the storage of deformation.

The SME process is closely related to the applied loading and temperature. To better understand the essence of the shape memory mechanism and optimize the processing of SMPs and SMP composites (SMPCs), it is important to establish constitutive models to provide theoretical guidance [8,9]. Currently, there are three methods to establish constitutive models for SMPs: the rheological modeling method, models based on the phase transition

concept, and a combination of the two models. For the rheological modeling method, a viscosity coefficient is introduced to account for time and temperature dependence, such that the model can describe the mechanical behavior of creep, relaxation, and rate dependence [10]. However, it cannot accurately describe the SME, limiting its predictability. The models based on the phase transition concept are more physically significant than the rheological models. It is assumed that SMPs are a type of composite consisting of different phases, which can transition between each other with temperature changes. This modeling method can reasonably explain the storage and release mechanisms of deformation and can easily obtain the model parameters. However, owing to specific assumptions, this modeling method is limited to the framework of the thermoelastic theory and cannot explain time- or temperature-related properties. These two modeling methods can complement each other; therefore, the last modeling method is a combination of the two.

Typically, by adding particles or fibers to the SMP matrix, the modulus and recovery force are improved. At present, the research of SMPC mainly focuses on material preparation, performance testing, and structural design, with limited theoretical research. However, to achieve intelligent and precise control of SMPC-based structures, it is important to suggest a reasonable theory to predict the mechanical response. For SMPCs, in addition to the thermodynamic properties of the matrix, the interaction between the fiber matrix and fiber should also be considered. Therefore, the thermodynamic constitutive and buckling models of SMPCs are more complex than those of SMPs.

This study integrates different modeling methods and discusses the representative constitutive models of SMPs and SMPCs. We review the theories of thermally actuated SMP from the rheological models, models based on the phase transition concept to the models combined with rheology and phase transition concept in Secs. 2–4. Furthermore, the constitutive models of the particulate-reinforced SMPCs, carbon-fiber-reinforced SMPCs, and buckling behavior of SMPCs are summarized in Sec. 5. Finally, in Sec. 6, we highlight the challenges in this field and provide an outlook on existing challenges and promising trends.

## 2 Rheological Model of Shape Memory Polymers

The schematics of rheological models typically contain several springs and dashpot elements, and different combinations represent the different main mechanical behaviors of the SMPs. This can clearly describe the underlying physical mechanism of SMPs in the amorphous state.

**2.1 Basic Viscoelastic Model.** Early studies employed the modified linear viscoelastic model to represent the thermodynamic behavior of SMPs. By introducing a sliding element into the standard linear solid (SLS) model, Tobushi et al. [11] proposed a four-element model for SMPs to describe the strain storage and release effect. This model was the starting point for the rheological model of SMPs, and significant effort has been made on this basis. Subsequently, Lin et al. [12] proposed a linear model for a polyurethane-based SMP, which consisted of two parallel Maxwell branches: one for the reversible phase and the other for the fixed phase. However, the model did not consider stress recovery and could not accurately predict the SME. Tobushi et al. [13] modified an earlier model and established a nonlinear model by introducing a nonlinear term. This model can be used to predict different thermodynamic behaviors within a 20% strain. A schematic of the model is listed in Table 1$a$, where $\varepsilon_s$ represents residual strain.

Abrahamson et al. (Table 1$b$) [14] and Morshedian et al. [15,16] established a constitutive model for SMPs employing a series model of the Kelvin and viscous elements. Bonner et al. [17] developed a Kelvin–Voigt-based theory and investigated the relationship between recovery time, recovery stress, and the fabrication process. However, only the stress relaxation behavior of the SMP was considered in this model. By introducing the

modified Maxwell–Weichert model, Heuchel et al. [18] proposed a constitutive model and predicted the stress relaxation of SMPs (Table 1$c$). Based on Tobushi's model, Li et al. [19] established a rheological method for low-strain conditions (Table 1$d$). The model effectively simulated the stress–strain-temperature relationship in the free and constrained recovery processes as follows:

$$\sigma + \frac{\mu(T)}{(E_1(T) + E_2(T))}\frac{d\sigma}{dt} = \frac{\mu(T)}{(1 + E_1(T)/E_2(T))}\left(\frac{d\varepsilon}{dt} - \alpha\frac{dT}{dt}\right)$$
$$+ \frac{1}{(1/E_1(T) + 1/E_2(T))}(\varepsilon - \alpha(T - T_0)) \tag{1}$$

where $E_1$ and $E_2$ denote the elastic moduli of the two spring branches, respectively, $\alpha$ the coefficient of thermal expansion, and $\mu$ the material parameter. This model type is simple to establish; however, the physical meanings of the model parameters are not sufficiently clear. In addition, it is challenging to describe a three-dimensional (3D) problem and the SME under a complex mechanical environment.

Diani et al. [20] determined that the crosslinked molecular network of SMPs could be deformed like an elastomer above its $T_g$ when the deformation is primarily driven by entropy change. The mechanical behavior of SMPs in the glassy state is mainly driven by internal energy. Combined with the finite deformation theory and SLS model, the authors developed the first 3D finite deformation constitutive model

$$\begin{cases} W = U(\mathbf{F}^e) - \eta_0 T(\mathbf{F}^\nu) \\ \boldsymbol{\sigma}^\eta = \frac{E^r}{6}\frac{T}{T_h}\mathbf{F}^e\mathbf{F}^{eT} - p\mathbf{I} \quad (\text{entropy} - \text{stress}) \\ \boldsymbol{\sigma}^U = \mathbf{L}^e[\ln(\mathbf{V}^e)] \quad (\text{internal energy} - \text{stress}) \end{cases} \tag{2}$$

where $\eta_0$ denotes the entropy and depends on the global deformation gradient. The internal energy is a function of the viscous deformation, $\mathbf{F}^\nu$, $p$ denotes a Lagrange multiplier dependent on boundary conditions, $E^r$ and $\mathbf{L}^e$ denote the Young's modulus and fourth-order elastic constant tensor of SMPs, and $T$ and $\mathbf{I}$ denote the temperature and unit tensor, respectively. This model can effectively predict the residual strain during the thermal–mechanical cycle. However, during constrained recovery, the stress-temperature theory curve differs significantly from that of the experimental results.

Wong et al. [21] proposed a one-dimensional (1D) constitutive model for SMPs that consisted of a spring, dashpot, and rubbery element (Table 1$e$) and characterized the isothermal recovery process during the thermal–mechanical cycle. The Arruda–Boyce eight-chain model was employed to describe the mechanical properties of the rubbery state. The Eyring model was employed to predict the thermodynamic behavior of the viscoplastic element. In addition to changes in the viscoelastic physical parameters and structural relaxation effects, Ghosh et al. [22] suggested that the hysteresis effect of the yield stress was another key factor affecting the thermodynamic properties of SMPs. Therefore, a four-element viscoelastic model including a friction element was proposed (Table 1$f$). Kelvin and spring elements were used to represent the stress responses above and below the $T_g$, respectively. The friction element was parallel to the Kelvin element to describe the storage and release of the strain, where $\varepsilon$, $E$, $\eta$, and $k$ denote the strain, spring stiffness, viscosity, and friction coefficient, respectively, and $p$ and $e$ denote the plasticity and elasticity, respectively. This model does not consider the structural relaxation mechanism but describes the shape recovery process of SMPs by establishing various phenomenological constitutive relations of friction elements. Subsequently, Ghosh et al. [23] extended this theory to 3D. Based on the same theoretical model framework, Ghosh et al. [24] extended the model to a finite deformation range. The dynamic equation can be expressed as

$$\overline{\mathbf{T}} = \overline{\mathbf{C}}_G \left( \overline{\mathbf{e}}_e - \overline{\alpha} \left( \overline{\theta} - \overline{\theta}_h \right) \mathbf{I} \right) \qquad \text{stress equation}$$

$$\overline{\mathbf{D}}_{ve} = \frac{1}{\overline{\eta}_G} \left( \| \overline{\mathbf{A}}_{ve}^{\text{dev,sym}} \| - \overline{k} \right) \frac{\overline{\mathbf{A}}_{ve}^{\text{dev,sym}}}{\| \overline{\mathbf{A}}_{ve}^{\text{dev,sym}} \|} \quad \text{flow equation} \tag{3}$$

where $\overline{\mathbf{T}}$ denotes the nondimensional stress, $\overline{\mathbf{D}}_{ve}$ denotes the viscoelastic flow rate, $\theta$ is the state variable, $\overline{\eta}_G$ represent the nondimensional viscosity, $\overline{k}$ is a variable relates to temperature and stress, $\overline{\mathbf{C}}_G$ is the isotropic glassy stiffness matrices, $\overline{\alpha}$ is the coefficient of thermal expansion, and $\mathbf{A}_{ve}$ is the thermodynamic driving force.

By connecting the SLS model in series to the storage and thermal strain elements, Balogun et al. [25,26] proposed a 1D viscoelastic model considering binding factors and further extended it to the 3D model (Table 1g). The 1D expression of this constitutive model can be expressed as

$$\dot{\varepsilon} = \frac{\dot{\sigma}}{E(T)} + \frac{\sigma}{\mu(T)} + \frac{\varepsilon}{\lambda(T)} + \dot{\varepsilon}_{th} + \dot{\varepsilon}_S \tag{4}$$

where $E$, $\mu$, and $\lambda$ denote the elastic modulus, viscosity, and delay time, respectively, and $\dot{\varepsilon}_{th}$ and $\dot{\varepsilon}_S$ denote the storage and thermal strain rates, respectively.

Chen et al. [27] proposed a rheological theory for SMPs based on the deformation gradient decomposition framework. They considered the thermodynamic coupling effect and nonlinear viscous flow law. The Mooney–Rivlin and Hencky models were employed to describe the mechanical behavior of the rubbery and glassy phases, respectively (Table 1h). The stress of each branch can be expressed as

$$\begin{cases} \sigma = \overline{\sigma}_A + \overline{\sigma}_B + p\mathbf{I} \\ \overline{\sigma}_A = \frac{2}{J} (C_{10} + I_1 C_{01}) \overline{\mathbf{B}}_M - \frac{2}{J} C_{01} \overline{\mathbf{B}}_M^2 \\ \overline{\sigma}_B = \frac{2\mu_B}{J} \mathbf{R}_B^e (\ln \mathbf{U}_B^e) \mathbf{R}_B^{et} \end{cases} \tag{5}$$

where $p = 3k \frac{\ln J}{J}$, $J = \det(\mathbf{F}_M)$, and $\overline{\sigma}_A$ and $\overline{\sigma}_B$ denote the stress of the rubbery and glassy phases, respectively.

Table 1 summarizes the schematics of the basic viscoelastic models mentioned above.

## 2.2 Multibranch Viscoelastic Model.
In the viscoelastic model, the fluidity of the polymer chain is directly related to the viscosity or relaxation time. Multibranch models have more advantages in capturing multiple relaxation processes in polymer systems. By considering two types of time- and temperature-related mechanisms, Nguyen et al. [28] proposed a theory that includes viscoelastic effects with structural and stress relaxations and viscoplastic flow induced by stress. Structural relaxation was used to describe the time-dependent evolution of SMPs from the nonequilibrium to equilibrium states, where the virtual temperature concept was introduced to represent the nonequilibrium effect. A constitutive model suitable for thermally induced amorphous SMPs was established by introducing the nonlinear Adams–Gibbs and Eyring viscoelastic models. The effective viscosity coefficient can be expressed as

$$\eta = \eta_0 \frac{Q}{T} \frac{s}{s_y} \exp \left[ \frac{C_1}{0.433} \left( \frac{C_2(T - T_f) + T \left( T_f - T_g^{ref} \right)}{T \left( C_2 + T - T_g^{ref} \right)} \right) \right]$$
$$\left[ \sinh \left( \frac{Q}{T} \frac{s}{s_y} \right) \right]^{-1} \tag{6}$$

where $\eta_0$ denotes the viscosity coefficient at the reference temperature $T_g^{ref}$; $T_f$ is the fictive temperature; $Q$ is the activation energy

parameter; $s$ is the flowing stress; $s_y$ is the isothermal shear stiffness to characterize the yield behavior of SMP; $C_1$ and $C_2$ are two parameters of the Williams–Landel–Ferry equation.

The viscosity equation describes viscosity as a function of time and temperature, which plays a key role in describing the SME. Furthermore, the viscous flow law can be expressed as

$$\dot{\gamma}^v = \frac{s_y}{\sqrt{2}\eta_0} \frac{T}{Q} \exp \left[ \frac{C_1}{0.433} \left( \frac{C_2(T - T_f) + T \left( T_f - T_g^{ref} \right)}{T \left( C_2 + T - T_g^{ref} \right)} \right) \right]$$
$$\left[ \sinh \left( \frac{Q}{T} \frac{s}{s_y} \right) \right] \tag{7}$$

However, it cannot describe the viscoplastic yield and fluid behavior at low temperatures. To address these problems, Xiao et al. [29] focused on viscous flow and yield behaviors below the $T_g$ and established a coupled thermodynamic framework (Table 2a). The expression for the total stress is as follows:

$$\sigma = \underbrace{\frac{1}{J} \frac{\mu_N}{3} \frac{T_f}{T_0} \frac{\lambda_L}{\overline{\lambda}_{eff}} \mathcal{L}^{-1} \left( \frac{\overline{\lambda}_{eff}}{\lambda_L} \right) \left( \overline{\mathbf{b}}_M - \frac{1}{3} \overline{I}_{M_1} \mathbf{1} \right)}_{S^{eq}}$$
$$+ \underbrace{\sum_{k=1}^{N} \frac{1}{J} \mu_k^{neq} \left( \overline{\mathbf{b}}_k - \frac{1}{3} \mathbf{I}_{1k}^e \mathbf{1} \right)}_{S^{neq}} + \underbrace{\frac{1}{2J} \kappa \left( J_M^2 - 1 \right) \mathbf{1}}_{P} \tag{8}$$
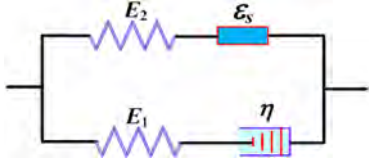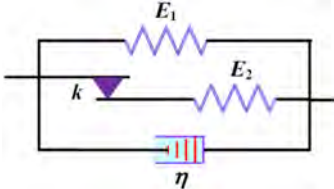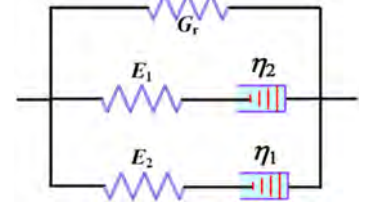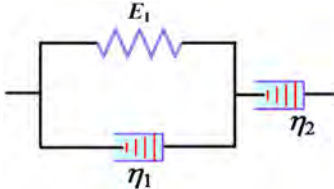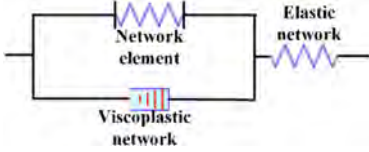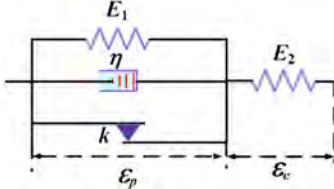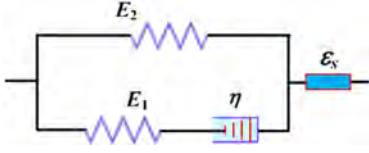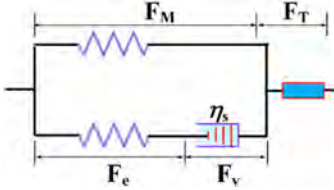
where $S^{eq}$, $S^{neq}$, and $\mathbf{P}$ denote the stress contributions of the equilibrium, nonequilibrium, and volumetric components, respectively. The equilibrium component was described by the Arruda–Boyce eight-chain model, and the nonequilibrium stress response was described by the Neo-Hookean model.

Buckley et al. [30] confirmed the significance of the viscoelastic relaxation spectrum using a genetic integral. Diani et al. [31] employed the generalized Maxwell model (GMM) to represent the discrete spectrum of relaxation time and the Williams–Landel–Ferry equation to describe the equivalence relationship between relaxation time and temperature. By introducing the Neo-Hookean model to describe the large deformation behavior, the model was extended to a finite deformation range. Twelve pairs of GMM parameters were obtained by a nonlinear fitting of the storage modulus and frequency curve. Arrieta et al. [32] successfully extended this modeling method to represent the free and constrained recovery under axial tension and high-strain conditions. Based on the viscoelastic and time–temperature equivalence principles, the shape memory behavior was predicted.

Anand et al. [33,34] developed finite deformation theories for thermoplastic SMPs. However, this type of model can only describe the mechanical behavior of SMPs below the $T_g$, significantly limiting its application. Srivastava et al. [35,36] established a thermoviscoelastic model of SMPs that coupled the heat transfer and generation effects in plastic deformation. In this study, the intermolecular resistance of the glassy state was represented by a Maxwell model, and an SLS model was employed to simulate the molecular network resistance (Table 2b). However, this study did not describe the relaxation mechanism. The relationships between the shear modulus, Poisson's ratio, and temperature were presented using a phenomenological theory. The model accurately described the rate- and temperature-dependent behaviors. However, it contains 45 parameters, the determination of which is tedious.

Referring to Nguyen's model, Li et al. [37] proposed a theory to simulate the thermal–mechanical process and obtain a temporary morphology below the $T_g$. The Narayanaswamy–Moynihan model was used to characterize the structural relaxation, and the dependence of the structure and stress relaxation time on the temperature was obtained. There are 17 parameters in this model, all of which were obtained from standard thermodynamic

**Table 1   Summary of the schematics of the basic viscoelastic model**

| | Schematics | References | | Schematics | References |
|---|---|---|---|---|---|
| a | | [13] | b | | [14] |
| c | | [18] | d | | [15,19] |
| e | | [21] | f | | [22] |
| g | | [25] | h | | [20,27] |

$\bigwedge\!\bigwedge$: spring element; ⊐|||⊏: dashpot element; $k$: microslip parameter; $E$: elastic modulus; $\eta$: material damping

experiments. Notably, unlike the previous SME, the temporary configuration of the SMP was obtained in the glassy state.

Westbrook et al. [38] developed a multibranch model to capture the SME (Table 2c). Two groups of nonequilibrium branches representing the glassy and rubbery states were introduced to describe the different relaxation modes, significantly reducing the material parameters. The influence of additional nonequilibrium rubbery branches on the overall prediction effect is discussed under different thermal and mechanical loading history conditions

$$\boldsymbol{\sigma} = \boldsymbol{\sigma}_{\text{eq}} + \boldsymbol{\sigma}_g + \sum_{i=1}^{m} \boldsymbol{\sigma}_r^i = \frac{nk_B T}{3J_M} \frac{\sqrt{N}}{\lambda_{\text{chain}}} \mathcal{L}^{-1}\left(\frac{\lambda_{\text{chain}}}{\sqrt{N}}\right)\overline{\mathbf{B}}' + \boldsymbol{\sigma}_g$$
$$+ K(J_M - 1)\mathbf{I} + \sum_{i=1}^{m} \frac{1}{J_e^i}\left[\mathbf{L}_e^i(T){:}\mathbf{E}_e^i\right] \qquad (9)$$

where $N$ is crosslinking density, $k_B$ is Boltzmann constant, and $T$ is temperature.

Yu et al. [39] proposed a 1D low-strain genetic integral model combined with a discrete relaxation time spectrum and simulated multiple SMEs. Subsequently, Yu et al. [40,41] constructed a 3D large-deformation constitutive model. Multirelaxation processes introduced multiple Maxwell elements, as shown in Table 2d, and investigated the determination method of material parameters through a series of experiments.

Sweeney et al. [42] proposed a viscoelastic model for SMPs by introducing three Maxwell element branches, in which the spring elements were expressed by the Neo-Hookean equation, and the dashpot elements were described by the Eyring equation. Ge et al. [43] proposed another model for predicting the free recovery of

SMPs. In addition to predicting the SME, it can characterize the rate dependence and relaxation behavior. Gu et al. [44] established a multibranch thermoviscoelastic model for SMP foams, which divided the deformation into the SMPs and elastic glass microspheres (Table 2e). The structural relaxation behavior above the $T_g$ is described using the Adams–Gibbs model. The multirelaxation process was described using the modified Eying viscous flow law. Table 2 summarizes the schematics of the multibranch viscoelastic model.

**2.3   Fractional Viscoelastic Constitutive Models.** Viscoelastic theory is an earlier and more commonly used method for describing the mechanical behavior of SMPs. Using this method, SMPs are regarded as a combination of springs, dashpots, and sliders, and series or parallel viscoelastic models are used to describe their thermodynamic properties. However, this type of model involves several parameters. Fractional viscoelastic constitutive models can describe the complex viscoelastic relationship that is difficult to describe in integer calculus, and the model parameters are less than in integer calculus; therefore, they have been widely employed to model the constitutive relationship of viscoelastic materials.

Several types of constitutive models for SMPs exhibit power-law relaxation behavior. Typically, the evolution of the relaxation modulus with time is described by the Prony series. Increasing the terms of the Prony series can improve the accuracy of the model; however, it also causes problems for subsequent calculations. Combined with the rheological theory, the fractional viscoelastic constitutive model can significantly decrease the number of material parameters. Currently, the description of the relaxation or complex moduli of SMPs typically employs the differential

**Table 2  Summary of the schematics of the multibranch viscoelastic model**

| | Schematics | References |
|---|---|---|
| *a* |  | Xiao et al. [29] |
| *b* |  | Srivastava et al. [36] |
| *c* |  | Westbrook et al. [38] |
| *d* |  | Yu [40] |
| *e* |  | Gu et al. [44] |

: spring element; : dashpot element; *E*: elastic modulus; $\eta$, $\tau$: material damping; TEC: thermal expansion component.

equation of an integer derivative, which is typically the serial and parallel form of the Kelvin or Maxwell models.

The first fractional derivative model was proposed by Nguyen et al. [45], as shown in Fig. 1, and the discrete spectrum was obtained by fitting the main curve of the storage modulus. Only two parameters were used in this model to describe the complex viscoelastic relationship, significantly decreasing the number of parameters.

Attempting to describe complex viscoelastic behaviors with fewer parameters, Fang et al. [46] employed the fractional-order Zener-type model to predict the mechanical response of SMPs. Combined with the SLS model, Li et al. [47] investigated the thermal–mechanical process of SMPs using the same method. Pan et al. [48] systematically investigated the thermodynamic behavior of SMPs by establishing a fractional viscoelastic model (Fig. 2). The entire model consisted of two fractional Maxwell
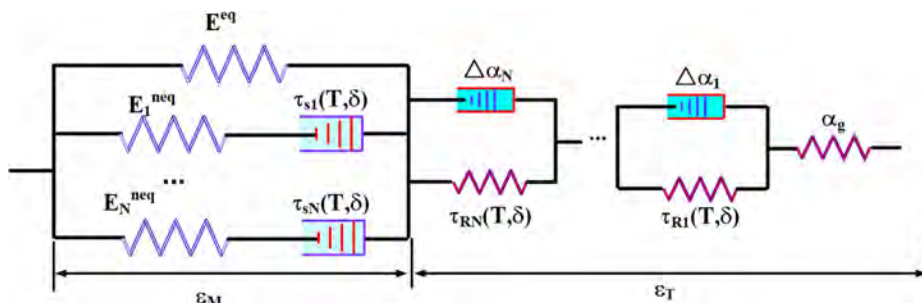
**Fig. 1 Schematic of the constitutive model developed by Nguyen et al.; $E^{eq}$ and $E^{neq}$ denote the elastic moduli of the equilibrium and nonequilibrium branches [45]**
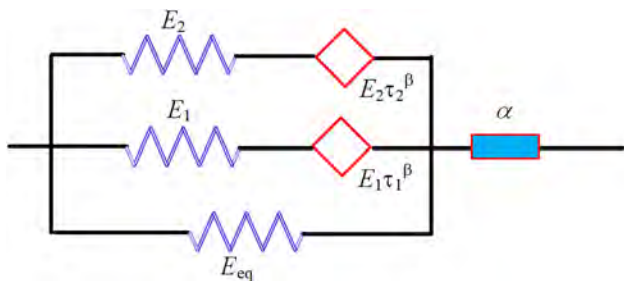


**Fig. 2 Fractional viscoelastic models proposed by Pan et al. [48]**

branches, a Hookean element branch, and a thermal expansion element branch, which can be expressed as

$$
\begin{aligned}
\sigma_M(t) &= \sigma_{eq}(t) + \sum_{i=1}^{m} \sigma_i(t) \\
&= E_{eq}\varepsilon_M(t) + \sum_{i=1}^{2}\left[ E_i \int_{t_0}^{t} E_\beta\left( -\left(\frac{(t-\xi)}{\tau_i}\right)^\beta \right) \frac{d\varepsilon_M(\xi)}{d\xi}d\xi \right. \\
&\quad \left. + E_\beta\left( -\left(\frac{t-t_0}{\tau_i}\right)^\beta \right)\sigma_i(t_0) \right]
\end{aligned}
\tag{10}
$$

where $E_\beta$ denotes the Mitting–Leffler equation, $\tau$ the relaxation time, and $\beta \in [0, 1]$. When $\beta = 0$, the spring-dashpot degenerates into a simple spring model, and when $\beta = 1$, the spring-dashpot degenerates into a simple Newton-dashpot model. The spring-dashpot element can characterize the properties of the material from the solid to fluid states, and eliminate the restriction that a component can only be a spring or a dashpot. This type of model can reflect the nonlinear gradual change process in the viscoelastic problem, and the model parameters have a clear physical significance.
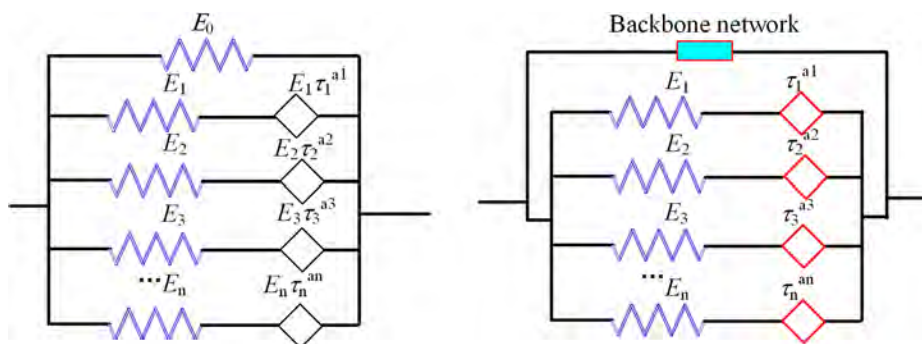
Combining the GMM and Maxwell–Wiechert models, Zeng et al. [49,50] constructed multirelaxation fractional thermoviscoelastic models, which can accurately predict the temperature-dependent free recovery process (Fig. 3). The fractional model can describe the relaxation or complex modulus with multiple orders of magnitude, or a wide range of frequency domains with fewer material parameters. Moreover, it is easier to obtain analytical solutions using Fourier or Laplace transforms.

## 3 Constitutive Model Based on the Phase Transition Concept

In this type of constitutive theory, SMPs are regarded as composites consisting of different phases, and the temperature change causes a variation in the volume ratio of each phase. This type of model describes the deformation mechanism by introducing the phase-transition concept from the perspective of entropy and energy change. However, because there is no physical phase transition in amorphous polymers, the thermodynamic process described by the phase-transition model is not a real process. Therefore, constitutive models based on the phase transition concept cannot clearly describe deformable storage owing to the weakening of the molecular fluidity during cooling. Although the physical meaning of the phase transition models is unclear, they also provide an effective method for predicting the SME.

Liu et al. [51] first established phase transition models for the 3D slight deformation of epoxy-based SMPs through a series of uniaxial experiments. Combined with the phase transition concept, the authors considered that the molecular chain of the active phase had a strong kinetic ability, and its deformation was achieved by a change in entropy. The kinematic ability of the molecular chains in the frozen phase was weak, and their deformation was achieved by a change in the internal energy. With a change in temperature, the SME was accompanied by a change in the volume fraction of the phases. Based on the uniform stress assumption, the same point in the matrix possesses the same stress before and after the glass transition.
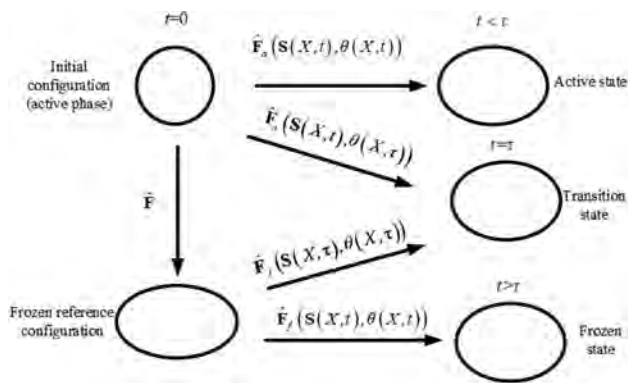


**Fig. 3 Multirelaxation fractional thermoviscoelastic models proposed by Zeng et al. [49,50]**

**Fig. 4 Evolution of the reference configuration in the phase transition process**

Using the volume fraction of the glassy phase as an internal variable, Chen et al. [52,53] further extended the phase transition method and established a 3D constitutive model for highly deformed SMPs. The freezing reference configuration was

introduced to calculate the freezing process of material particles in different periods. Furthermore, the author suggests that the glassy and rubbery phases exhibited the same mechanical response, and the frozen strain completely recovered after heating up. This model is established in the framework of the existing nonlinear viscoelastic constitutive theory, without explicitly considering the intermolecular interactions. Figure 4 illustrated the evolution of the reference configuration during the phase transition. During cooling, the active, frozen, and phase transition intermediate states exist simultaneously in the polymer. During the transition from the active to phase transition intermediate states, the strain changes from $\hat{\mathbf{F}}_a(t)(\mathbf{S}(t),\theta(t))$ to $\hat{\mathbf{F}}_a(t)(\mathbf{S}(\tau),\theta(\tau))$. $\tau$ denotes the phase transition time. When $t < \tau$, the material is in the active state; when $t > \tau$, the material completes the phase transformation and moves to the frozen state; when $t = \tau$, the material is undergoing a phase transition. During the transition from the active to frozen states, the material satisfies $\mathbf{F}(X, \tau + 0) = \hat{\mathbf{F}}_f(\mathbf{S}(X, \tau), \theta(X, \tau))\overline{\mathbf{F}}$. Furthermore, to ensure the continuity of material deformation, the material satisfies $\hat{\mathbf{F}}_a(\mathbf{S}(x, \tau), \theta(x, \tau)) = \hat{\mathbf{F}}_f(\mathbf{S}(X, \tau), \theta(X, \tau))\overline{\mathbf{F}}$. Consequently, during the constant strain-cooling process, the deformation distribution inside SMPs can be expressed as follows:

$$\mathbf{F}(X,t) = \begin{cases} \hat{\mathbf{F}}_a(\mathbf{S}(X,t),\theta(X,t)); & \text{if } X \notin \Omega_f \theta(X,t) \\ \hat{\mathbf{F}}_f^{-1}(\mathbf{S}(X,\tau),\theta(X,\tau))\hat{\mathbf{F}}_f(\mathbf{S}(X,t),\theta(X,t))\hat{\mathbf{F}}_a(\mathbf{S}(X,\tau),\theta(X,\tau)); & \text{if } X \in \Omega_f \theta(X,t) \end{cases} \quad (11)$$

Considering that the transformation process is rate-dependent, Pan et al. [54] proposed another phase evolution equation. By studying the crystallization process of SMPs, Rao et al. [55] established a constitutive equation to simulate the thermal–mechanical process of crystallized SMPs. This model describes the SME and the transition between the formation and melting of the crystal phase. The uniaxial cyclic deformation and nonuniform shear deformation of the hollow cylinder were investigated using this model. The stress of the semicrystalline phase is expressed as follows:

$$\mathbf{T} = -p\mathbf{I} + (1 - \alpha)2\rho\mathbf{F}_{\kappa_a}\frac{\partial\psi_a}{\partial C_{\kappa_a}}\mathbf{F}_{\kappa_a}^T + \alpha2\rho\mathbf{F}_{\kappa_c}\frac{\partial\psi_c}{\partial C_{\kappa_c}}\mathbf{F}_{\kappa_c}^T$$
$$= -p\mathbf{I} + (1 - \alpha)\hat{\mathbf{T}}_\mathbf{a} + \alpha\hat{\mathbf{T}}_\mathbf{c} \quad (12)$$

where $\mathbf{T}$ denotes the average stress of the material, $\hat{\mathbf{T}}_\mathbf{a}$ the amorphous stress, $\hat{\mathbf{T}}_\mathbf{c}$ the stress of the crystalline phase, $C_{\kappa_a}$ and $C_{\kappa_c}$ the right Cauchy–Green tensor, $\mathbf{F}_{\kappa_a}$ the deformation gradient in the fixed configuration, and $\psi$ the Helmholtz energy. Subsequently, Rao et al. [56] modified the model and proposed a complete constitutive model for the thermodynamic framework. This model provided the constitutive relations of the rubbery (amorphous phase) and semicrystalline phases. Volk et al. [57–60] proposed a series of constitutive models combined with the Neo-Hookean model and a hyperbolic tangent function for different mechanical behaviors of SMPs. The Neo-Hookean equation was used to represent the mechanical behavior of the active phase, whereas the hyperbolic tangent function was used to characterize the mechanical behavior of the frozen phase.

The phase evolution model typically makes certain assumptions to simplify the calculation. Liu et al. [51] and Chen et al. [52] employed the uniform stress hypothesis, indicating that the active and frozen phases have the same stress. Qi et al. [61] assumed that the initial frozen and active phases have the same strain. Further, Gilormini et al. [62] investigated various homogenization

hypotheses, including the uniform strain hypothesis, uniform stress hypothesis, and Hashin–Shtrikman upper and lower boundary approximations. The results indicate that the predictive ability of these uniform hypotheses did not differ significantly. The predictability of the uniform strain hypothesis is better than that of the uniform stress hypothesis. The more complex self-consistent approximation and the Hashin–Shtrikman upper and lower boundaries did not significantly improve the predictability compared with the strain hypothesis.

By investigating the evolution rules of the glassy phase, Kazakeviciute–Makovska et al. [63] determined that they correlated well with the free-recovery experimental data when various prestrains were normalized as the main curve. Moreover, they noted that the current methods for determining the volume fraction and predicting the stress responses of constraint restoration were not ideal. They developed a new evolution model for the glassy phase volume fraction by introducing additional temperature-dependent parameters.

Combined with the second law of thermodynamics, Baghani et al. [64] proposed a 3D model by assuming that SMPs are composites of active and frozen phases (Fig. 5) that can be converted to each other by external thermal stimulation. Utilizing the first-order mixing rule, the deformation was divided into the thermal, initial frozen phase, new frozen phase, and stored strains. By analyzing the changes in the physical parameters during the loading process, the evolution law of the internal variables was obtained.
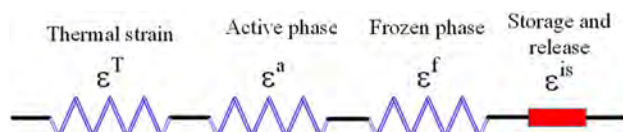


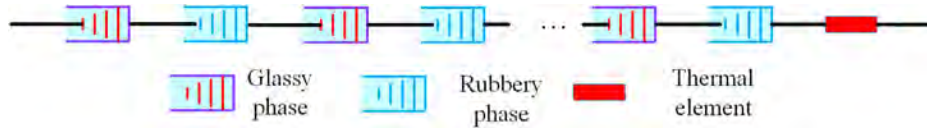**Fig. 5 Constitutive model proposed by Baghani et al. [65]**

**Fig. 6 Schematic of the model proposed by Li et al.**

Using a rectangular bar and a circular tube as examples, the torsion behavior was simulated, and the validity of the model was verified. However, this model is applicable only to slight deformations. Baghani et al. [65] extended this model and developed a 3D finite deformation model. The free energy can be expressed as

$$\Psi(\varepsilon, \mathbf{T}, \varphi^r, \varphi^g, \varepsilon^r, \varepsilon^g, \varepsilon^s) = \varphi^r \Psi^r(\varepsilon^r) + \varphi^g \Psi^g(\varepsilon^g)$$
$$+ \Psi^\lambda(\varepsilon, \mathbf{T}, \varphi^r, \varphi^g, \varepsilon^r, \varepsilon^g, \varepsilon^s) + \Psi^T(T) \quad (13)$$

where $\Psi$ denotes the Helmholtz free energy density function, $\varphi$ the volume fractions of each phase, $r$, $g$, and $T$ the rubbery phase, glassy phase, and thermal symbol, respectively, $\varepsilon^s$ the storage strain, and $\Psi^\lambda$ a kinematic constraint.

Assuming that SMPs are a type of particle composite, Yang et al. [66] proposed a constitutive model combined with the Mori–Tanaka theory and a new phase evolution equation. Assuming that the phase evolution process occurred in stages, Li et al. [67] proposed a constitutive model for SMPs. In this model, the formation of the frozen phase was independent of the heating and cooling rates. Subsequently, Li et al. [68] modified this model and proposed another phase-evolution equation by introducing time factors. In this study, the concept of the frozen strain rate is introduced. It is assumed that when the temperature change is $\Delta T$, and the time, $\Delta t$, is sufficient, the phase transformation can be completed, and the frozen strain, $\Delta \varepsilon_{f-\text{real}}$, equals the theoretical value, $\Delta \varepsilon_f$. Else, the actual value of $\Delta \varepsilon_{f-\text{real}}$ is less than the theoretical value, $\Delta \varepsilon_f$. Consequently, the expression for the freezing strain, $\Delta \varepsilon_{f-\text{real}}$, is a function of time. The transition between the two phases is assumed to be a continuous process (Fig. 6). For this model, the critical formula can be expressed as

$$\begin{cases} \sigma_{\text{total}} = \dfrac{\varepsilon_{\text{total}} - \varepsilon_{f-\text{real}} - \varepsilon_T}{\dfrac{\gamma}{E_g} + \dfrac{1-\gamma}{E_r}} \\ \dfrac{d\varepsilon_f}{dT} = \dfrac{d\gamma}{dT} \left[ 1 - f(T) \right] \dfrac{\varepsilon_{\text{total}} - \varepsilon_f - \varepsilon_T}{E_r \left( \dfrac{\gamma}{E_g} + \dfrac{1-\gamma}{E_r} \right)} \\ \varepsilon_{f-\text{real}} = \varepsilon_f - \displaystyle\int_0^t \dot{\varepsilon}_f e^{\frac{-(t-a)}{\tau}} da \end{cases} \quad (14)$$

where $\varepsilon_T$ denotes the thermal strain, $\gamma$ the internal variable fraction of the glassy phase, $E_g$ and $E_r$ the elastic moduli of the glassy and rubbery phases, respectively, $\varepsilon_f$ the theoretical frozen strain, and $\varepsilon_{f-\text{real}}$ the actual frozen strain.

Assuming that the phase transition is caused by internal stress, Lu et al. [69] developed a constitutive theory related to the internal stress concept. Arvanitakis et al. [70] proposed a phase transition equation for thermosetting materials based on the level-set method. The phase transition model is simple to construct and widely applicable and can be applied to describe the constitutive relations of various SMPs and SMPCs. For semicrystalline SMPs, the physical significance of the phase transition model is clear. The material separation phase of semicrystalline SMPs is divided into amorphous and crystalline regions, and the generation of the phase transition is accompanied by melting and crystallization. However, for amorphous polymers, the phase transition is conceptual and has no physical significance; therefore, it is impossible to obtain the true volume fraction of each phase. The commonly used method employs free recovery data under specific prestrain

conditions to determine the volume fractions of each phase. The free recovery experiments under other prestrain conditions were then used to test the rationality of such volume fractions. However, although the obtained model fits well with the experimental results, there is no specific physical significance.

## 4 Viscoelastic Models Combing Rheology and Phase Transition Concept

Phase evolution models are simple to establish, but they lack physical significance. The model parameters cannot be obtained from standard thermodynamic experiments. The rheology modeling method is more versatile and practical; however, this type of model is more complex, and several parameters need to be determined. The predictability of the phase transition theory or rheological model alone is limited. Consequently, a new framework is established by combining the viscoelastic and phase transition theories.

Qi et al. [61] first established a 3D finite deformation constitutive model for the complex multi-axial thermodynamic behavior of amorphous SMPs by combining the viscoelastic model and phase transition concept. In this study, SMPs are assumed to comprise rubbery, initial glassy, and frozen glassy phases. The mechanical properties of the rubbery and initial glassy phases were described by the Arruda–Boyce eight-chain and thermoviscoelastic models, respectively. The definition of the transformation gradient of the frozen phase is key to expressing the SME in this model. The model contains 17 parameters, including eight for the stress of the elastic part, seven for the viscoplastic part, and two for the Vogel–Tammann–Fulcher function of the frozen phase volume fraction. The deformation gradient and corresponding free-energy equations are as follows:

$$\mathbf{T} = f_r \mathbf{T}_r + f_{g0} \mathbf{T}_{g0} + f_T \mathbf{T}_T \quad (15)$$

where $f_r$, $f_{g0}$, and $f_T$ denote the volume fractions of the rubbery, initial glassy, and frozen glassy phases, respectively, and $\mathbf{T}_r$, $\mathbf{T}_{g0}$, and $\mathbf{T}_T$ correspond to their Cauchy stresses, respectively. For the stress tensor, $\mathbf{T}_T$, of the frozen glassy phases, Qi et al. suggested that the deformation was the redistribution of the overall deformation, and it was assumed that all frozen glassy phases had the same deformation gradient at different times. Consequently, there is an increment, $\Delta \mathbf{F}_T^{n+1}$, of the deformation gradient of the frozen glass phase

$$\Delta \mathbf{F}_T^{n+1} = \begin{cases} \mathbf{F}^{n+1} (\mathbf{F}^n)^{-1} & \text{if } \Delta T \neq 0 \\ \mathbf{I} & \text{if } \Delta T = 0 \end{cases} \quad (16)$$

where $\mathbf{F}^n$ and $\mathbf{F}^{n+1}$ denote the global deformation gradients of the increment from $n$ to $n+1$, respectively. Although the model can accurately simulate the SME of SMPs, the form of the constitutive model is complex because several other classical models have been incorporated into the modeling process.

By analyzing the microstructure of SMPs, Kim et al. [71] established a 1D constitutive theory that contained one viscoelastic hard phase and two hyperelastic soft phases. The two soft phases corresponded to the mechanical behavior of SMPs in the rubbery and glassy states, which were represented by the Mooney–Rivlin hyperelastic model, whereas the hard phase is described by a linear viscoelastic model (Fig. 7). In this study, the SLS model was used to describe the mechanical behavior of the hard phase, and
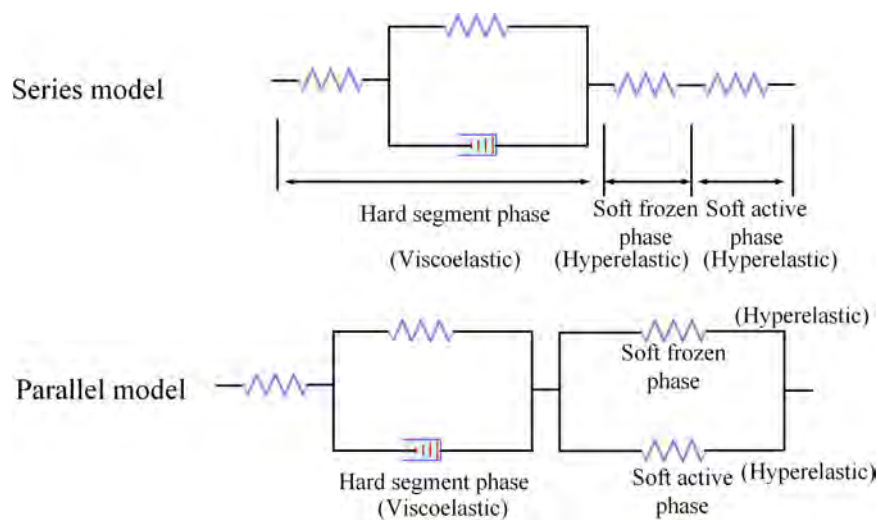
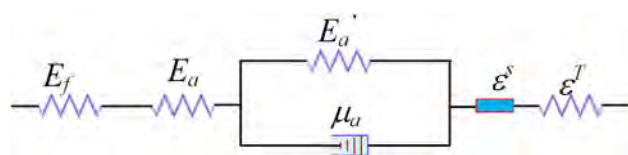**Fig. 7 Schematic of the series model and the parallel model**



**Fig. 8 Schematic of the phase evolution model**

the following genetic integral form was applied to the constitutive relation of the model:

$$\sigma_{\mathrm{h}} = \sigma_s = \int_t Y(t-\tau)\frac{d\varepsilon}{d\tau}d\tau \qquad (17)$$

where the relaxation modulus satisfies: $Y(t-\tau) = q_0 + (q_1/p_1 - q_0)\exp(-t/p_2)$, $p_1 = \mu(E_1+E_2)$, $q_0 = \frac{E_1 E_2}{E_1+E_2}$, $q_1 = \frac{E_1\mu}{E_1+E_2}$.

For the soft phases that contain the frozen phase and active phase, the Mooney–Rivlin model was used to describe the mechanical behavior, which can be expressed as

$$\sigma_{\mathrm{u}} = 2C_{10}(\lambda_u - \lambda_u^{-2}) + 2C_{10}(1-\lambda_u^{-3}), \quad \lambda_u = 1+\varepsilon_u \qquad (18)$$

where $\sigma_u$, $\varepsilon_u$, and $\lambda_u$ denote the stress, strain, and axial elongation ratios, respectively.

The model parameters were determined by differential scanning calorimetry (DSC) experiments and a series of tensile tests at different temperatures. The parallel model was significantly affected by the tensile properties, whereas the series model was more susceptible to the strain storage rate. However, from the series and parallel hypotheses of the model, it can be observed that the deformation mechanism of the SMPs remained in the conjecture stage.

Based on this model, Gu et al. [72] used the affine network model to replace the Mooney–Rivlin model to characterize the change rule for the soft segment and proposed a 3D constitutive model. Combined with the phase transition concept, Wang et al. [73] proposed a physical, temperature, and time-related

constitutive model for SMPs. By assuming it to be a composite, the Mori–Tanaka theory was introduced to describe the mechanical behavior of SMPs. The stress is expressed as

$$\sigma = \tilde{\mathbf{L}}(\varepsilon - \varepsilon_f^M - \varepsilon_f^T) = \tilde{\mathbf{L}}[\varepsilon^{\mathrm{pre}}(1-\Phi_f^M) + \varepsilon^T(1-\Phi_f^T)] \qquad (19)$$

where $\varepsilon^{\mathrm{pre}}$ denotes the prestrain, $\Phi_f^M$ and $\Phi_f^T$ the fractions of the mechanical and thermal parts of the frozen phase, respectively, $\tilde{\mathbf{L}}$ can be obtained by $\tilde{\mathbf{L}} = \mathbf{L}_{\mathrm{a}}(\mathbf{I} + \Phi_f\mathbf{A})^{-1}$, and $\mathbf{L}_{\mathrm{a}}$ denotes the stiffness tensor of the active phase.

Reese et al. [74] proposed a thermodynamically coupled model to describe the mechanical behavior of the rubbery state from macroscopic and mesoscopic perspectives. Using a finite element approach, they developed a tetrahedral cell to simulate the rubbery phase. Subsequently, the constitutive models were inserted into finite element software to analyze the two-dimensional (2D) and 3D thermodynamic problems. Using this model, the SME of the two types of vascular stent structures was simulated, and its validity was verified. However, the viscoelastic behavior during the phase transition and inelastic effect of the two phases were not considered in this model.

Guo et al. [75] extended the traditional linear phase transition theory to nonlinear and established a normally distributed phase evolution model. According to the phase transition theory, the deformation was divided into three parts: the active phase strain, $\varepsilon^a$; frozen phase strain, $\varepsilon^f$; and thermal strain, $\varepsilon^T$ (Fig. 8).

Based on the phase transition theory, Guo et al. [76] investigated the strain hardening of SMPs by introducing a strain-rate parameter into the viscoelastic model. In another study, Guo et al. [77] assumed that during the phase transition process, SMPs comprise of a frozen state and several active states. Each phase state was characterized by a series of Kelvin and Maxwell elements (Fig. 9). During cooling, the active phase (element $i$), represented by the small viscous element, completes the phase transformation to the frozen state, and the strain in element $i$ is frozen and converted to the stored strain. The strain value of the SMPs at time $t$ under unit stress is a function of the temperature and time, which can be expressed as
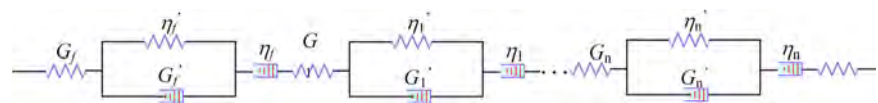


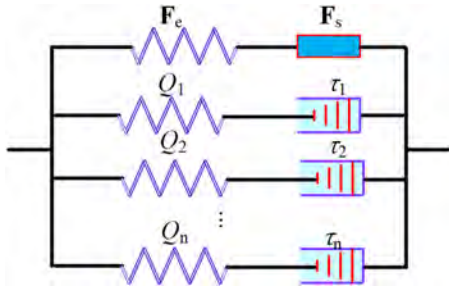**Fig. 9 Schematic of the phase evolution model**

**Fig. 10    Schematic of the phase evolution model**

$$\varepsilon = \phi_f(\varepsilon_s + \varepsilon_f^m) + \sum_1^n \phi_i \varepsilon_i^m + \varepsilon^T$$

$$= \sigma(\phi_f(T)J_f(T,t) + \sum_1^n \phi_i(T)J_i(T,t)) + \phi_f \varepsilon^s + \varepsilon^T \quad (20)$$

with $J_f(T,t) = \frac{1}{G_f} + \frac{1}{G_f'}(1 - e^{-\frac{t}{\tau_f}}) + \frac{t}{\eta_f}$ and $J_i(T,t) = \frac{1}{G_i} + \frac{1}{G_i'}$ $(1 - e^{-\frac{t}{\tau_i}}) + \frac{t}{\eta_i}$. where $G_i$ denotes the transient elastic modulus of the $i^{\text{th}}$ phase inside the SMP, the viscosity coefficient, $\eta_i$, is used to characterize the viscoelastic properties of the $i^{\text{th}}$ phase, $G_i'$ denotes the elastic modulus employed to characterize the viscoelastic behavior of polymer materials before and after the phase transition temperature, and $J_i(T,t)$ denotes the creep compliance.

This equation gives the constitutive equation describing the mechanical behavior of SMPs during each stage of deformation. During the loading process at a constant temperature, there was no phase transition process caused by the temperature, and the macroscopic performance was viscoelastic. The viscoelastic model can accurately describe the mechanical behavior of SMPs at different temperatures, and the introduction of the phase-transition volume fraction enables it to explain the shape-memory properties of SMPs.

Combining the rheological theory and phase evolution concept, Scalet et al. [78] developed a constitutive model for semicrystal SMP containing 14 parameters. Park et al. [79] developed a finite strain constitutive theory by dividing SMPs into active and frozen phases (Fig. 10). Both the rubbery and glassy phases were modeled using a visco-hyperelastic equation. The deformation gradient was multiplicatively divided into the deformation gradient of each phase to describe the deformation behavior of SMPs. However, this model can only predict the strain recovery process. Combined with the internal state variable modeling method, Bouaziz et al. [80] developed a new phase evolution equation. During heating and cooling, the temperature is transferred from the surface to the interior. Guo et al. [81] suggested that the phase evolution process followed the same rule and developed a constitutive model by considering the microstructure of semicrystalline SMPs.

Li et al. [82] developed a time-dependent viscoelastic model combined with the phase transition theory. Under an external load, the molecular network was crosslinked and redirected, and reversible phases (secondary crosslinking) formed during cooling, locking the deformed shape while disappearing during the heating process. The rubbery state was considered as an anisotropic incompressible material, and stress relaxation and creep under continuous loading were considered. When $T > T_g$, two incompressible spring elements and a dashpot element were employed to represent the mechanical behavior of the rubbery phase as shown in Fig. 11, and the total Cauchy stress, $\sigma$, can be expressed as $\sigma = \sigma_{R1} + \sigma_{R2}$. When $T < T_g$, a new reversible phase (secondary crosslinking) was activated, acting as a lock of the temporary shape, which was represented by a spring element in parallel with a viscous damper, and the Cauchy stress was calculated as $\sigma = \sigma_{R1} + \sigma_{R2} + \sigma_{E1} + \sigma_{E2}$.
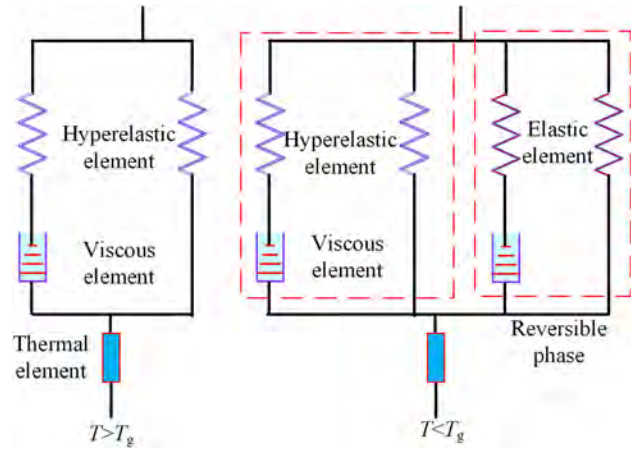
**Fig. 11    Schematic of the constitutive model**

Zhao et al. [83] proposed a constitutive model based on multiple decompositions of the deformation gradient. Combining the phase transition concept, SMPs were considered to be a composite consisting of glassy and rubbery phases (Fig. 12).

The advantage of viscoelastic models combined with the rheology and phase transition concept lies in their versatility and viability. They can describe the thermal-mechanical properties related to the temperature and rate without knowing the specific polymer network structure of the SMP. However, this type of model is complex and contains several parameters.

Table 3 summarizes the phase evolution equations. The determination of the volume fraction is an important part of the phase transition model. However, in the past phase volume fractions have been determined using empirical formulas because of the lack of reasonable physical interpretations. In theoretical models of the phase transition, SMPs are typically divided into two parts: the active and frozen phases. With increasing and decreasing temperatures, the phase transition between the active and frozen phases begins accompanied by the storage and release of strain, exhibiting the SME at the macrolevel. Therefore, a reasonable and accurate characterization of the variation in the volume fraction of the active or frozen phases with temperature is the key to explaining the SME using this model.
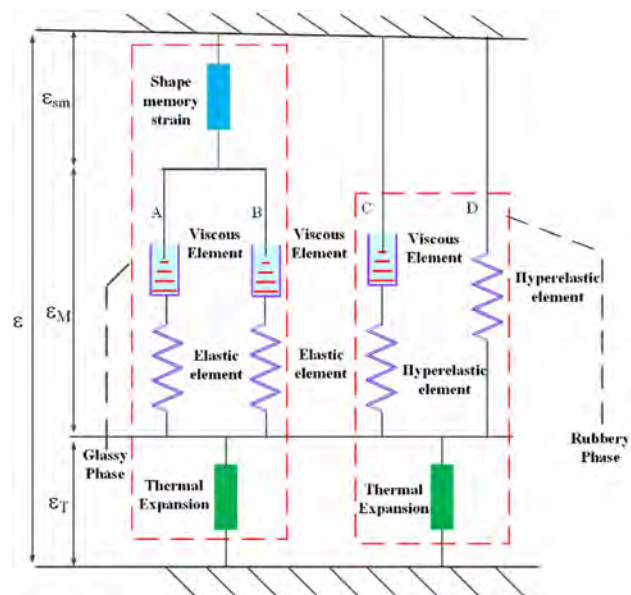


**Fig. 12    Schematic of the constitutive model proposed by Zhao et al.**

**Table 3    Summary of phase evolution equations**

| Phase evolution equations | References | Phase evolution equations | References |
|---|---|---|---|
| $\phi = 1 - \dfrac{1}{1 + c_f (T_h - T)^n}$ | Liu et al. [51] | $\phi_f = 1 - \dfrac{1}{1 + \exp\left(-\dfrac{T - T_t}{A}\right)}$ | Qi et al. [61] |
| $\phi = \alpha\exp\left(-\left(\dfrac{T_t}{T}\right)^m \beta^{-n}\right)$ | Wang et al. [73] | $\phi = \dfrac{1}{1 + \exp\left(\dfrac{2w}{T - T_t}\right)}$ | Reese et al. [74] |
| $\phi = \dfrac{b - \tanh((T - A)/B)}{b - a}$ | Volk et al. [58] | $\phi = \dfrac{1}{V}\displaystyle\int_\Omega \dfrac{1}{2}(I + \tanh(\psi/s))dV$ | Arvanitakis [70] |
| $\phi = \displaystyle\int_{T_s}^{T} \dfrac{1}{S\sqrt{2\pi}}\exp\left(-\dfrac{(T - T_g)^2}{2S^2}\right)dT$ | Guo et al. [75] | $\xi_g = \dfrac{b}{1 + \exp(c(T - T_{tr}))} - d$ | Park et al. [79] |
| $\phi = 1 - \dfrac{1}{1 + \exp\left(-\dfrac{T - T_{tr}(\dot{T})}{b}\right)}$ | Pan et al. [48] | $\gamma = 1 - \dfrac{1}{1 + c(T_h - T)^n} = \dfrac{\varepsilon_f}{\varepsilon_{\text{total}}}$ | Li [68] |

| Phase evolution equations | References |
|---|---|
| $\phi = \dfrac{1}{V}\displaystyle\int_\Omega \dfrac{1}{2}(I + \tanh(\psi/s))dV$ | Arvanitakis [70] |
| $\phi_f = \begin{cases} 0; & T < T_{\min} \\ \left(1 - \left(\dfrac{T - T_{\min}}{T_{\max} - T_{\min}}\right)^m\right)^n; & T_{\min} \leq T \leq T_{\max} \\ 1; & T > T_{\max} \end{cases}$ | Gilormini [62] |
| $\phi = 1 - \left(\displaystyle\int_{r_c(T)}^{\infty} p(r)dr\right) \times \left(1 - \left(1 - \exp\left(-\dfrac{\Delta H_a(T)}{k_B T}\right)\right)^{\frac{\Delta t}{\tau_0}}\right)$ | Yang and Li [66] |
| $\phi_f = 1 - \dfrac{1 - b}{1 + \exp(-a_1(T - T_r))} - \dfrac{b}{1 + \exp(-a_2(T - T_c))}$ | Bouaziz et al. [80] |
| $\xi^c = \begin{cases} \dfrac{1}{1 + \exp[\beta_{\text{cool}}(T - T_{c,\text{eff}})]} & \text{if } \dot{T} \leqslant 0 \\ \dfrac{1}{1 + \exp[\beta_{\text{cool}}(T_{END} - T_{c,\text{eff}})]}\dfrac{1}{1 + \exp[\beta_{\text{heat}}(T - T_{m,\text{eff}})]} & \text{if } \dot{T} \geqslant 0 \end{cases}$ | Scalet et al. [78] |
| $\phi = 1 + \dfrac{\tanh(\gamma_1 T_g - \gamma_2 T) - \tanh(\gamma_1 T_g - \gamma_2 T_h)}{\tanh(\gamma_1 T_g - \gamma_2 T_h) - \tanh(\gamma_1 T_g - \gamma_2 T_l)}$ | Baghani et al. [65] |
| $1 - \varphi_f = \varphi\exp(-(kT_{\text{tran}}/(T - \tau\beta))^m/\beta^n)$ | Guo et al. [81] |
| $\varphi_f = 1 - \gamma = 1 - AT\exp\left(-\dfrac{\Delta G(T_h)10^{\left(-\frac{C_1}{C_2 + T - T_h}\right)}}{RT} + \dfrac{T_h - T}{b \cdot T_h - T}\right)$ | Lu et al. [68] |

Typically, there are two methods to define storage strain: directly defining the expression of storage strain, such as the model of Park et al. [79], and deriving the evolution equation of storage strain, such as the model of Liu et al. [51]. Furthermore, some models do not define the stored strain but obtain the shape memory strain by a special strain relationship, such as the model of Qi et al. [61].

As exemplified by the phase-transition model proposed by Liu et al. [51], the variation in the frozen phase volume fraction with temperature can be expressed as

$$\phi_f = \frac{\varepsilon^*}{\varepsilon_{\text{pre}}} = 1 - \frac{1}{1 + c_f (T_h - T)^n} \tag{21}$$

where $\varepsilon^*$ denotes the storage strain, $\varepsilon_{\text{pre}}$ the prestrain of the SMP, and $c_f$ and $n$ are obtained by fitting the experimental data. The form of the model is simple, however, $c_f$ and $n$ have no physical significance, and are difficult to determine experimentally. In the

model proposed by Qi et al. [61], the variation in the frozen phase volume fraction can be expressed as

$$\phi_f = 1 - \frac{1}{1 + \exp\left(-\dfrac{T - T_r}{A}\right)} \tag{22}$$

where A denotes a constant highly dependent on the phase transition region of the material, and $T_r$ a characteristic temperature of the phase transition with a value approximately equal to the $T_g$. In 2012, Gilormini et al. presented a piecewise function model to describe the phase transition of SMPs, which can be expressed as

$$\phi_f = \begin{cases} 0; & T < T_{\min} \\ \left(1 - \left(\dfrac{T - T_{\min}}{T_{\max} - T_{\min}}\right)^m\right)^n; & T_{\min} \leq T \leq T_{\max} \\ 1; & T > T_{\max} \end{cases} \tag{23}$$

where $T_{\min}$ and $T_{\max}$ denote the initial and final temperatures of the phase transition, respectively. Compared with the experimental results, these three models can accurately characterize the phase transition behavior between the frozen and active phases. However, the models contain several parameters, which have no clear physical significance and can only be obtained by fitting the experimental results.

Furthermore, Guo et al. proposed a normal-distribution phase transition model to characterize the change in the volume fraction of the frozen phase

$$\phi = \int_{T_s}^{T} \frac{1}{S\sqrt{2\pi}} \exp\left(-\frac{(T-T_g)^2}{2S^2}\right) dT \qquad (24)$$

where the variance, $S$, can be expressed as $S = \frac{T_f - T_g}{n}$. The initial temperature, $T_s$, and finishing temperature, $T_f$, of the phase transformation, and phase-transition temperature, $T_g$, can be obtained by DSC experiments. The parameter, $n$, can be given by the boundary conditions under ideal conditions, that is, $\phi_f(T_{\min}) = 1$ and $\phi_f(T_{\max}) = 0$. By comparing the experimental and simulation results, it was determined that the normal distribution model can accurately characterize the variation in the frozen volume fraction with temperature during the phase transformation.

Each of the three types of SMP models has unique characteristics, and the modeling method chosen to describe the mechanical behavior requires consideration of which performance aspect to focus upon. For the phase transition model, SMPs are considered to be a mixture of glassy and rubbery phases. Under this classification, models have been established by Liu et al. [51], Chen and Lagoudas [52,53], and Pan et al. [54]. The phase transition models have sufficient flexibility in extending existing constitutive models of polymers to the rubbery and glassy phases to describe the SME. However, because the temperature variation rate and time hysteresis effect are not considered in this model, the thermal deformation related to the time–temperature course cannot be accurately described. For example, owing to the lack of time–temperature-related parameters to describe the change in mechanical properties in the model, the typical viscoelastic properties of the viscoelastic materials, such as relaxation, creep, and rate dependence, cannot be described.

For the rheological model, it can be observed that the viscoelastic model is extended to the thermodynamic behavior undergoing glass transition, and the viscosity parameters are regarded as nonlinear functions of temperature, as in the models established by Tobushi et al. [13], Nguyen et al. [28], Diani et al. [31], Li et al. [37], and Yu et al. [40,41]. The SME is considered to be due to the change in viscosity or relaxation time in the glass transition region caused by temperature changes. Compared with the phase transition model, the viscoelastic model does not directly describe the SME but describes the time-dependent mechanical properties of SMPs. Consequently, several time–temperature-related parameters in the model describe the changes in mechanical properties. However, a deeper physical explanation of the description of the SME is not provided. There are also no clear physical definitions of the storage and shape memory strains, which can only be described in phase-transition models. Therefore, such models cannot adequately explain the SME mechanism.

# 5 Constitutive Models of Shape Memory Polymers Composites

Typically, SMPs exhibit a low modulus and recovery force, and their practical applicability is low. Therefore, it is necessary to add reinforcing fillers to expand its application range. The fillers can be divided into particles and fibers, including short fibers, unidirectional continuous fibers, and woven fiber cloths. SMPCs need to add a theoretical description of the interaction between the reinforcing phase and matrix, and between the reinforcing phase and reinforcing phase by considering the complex thermodynamic characteristics of the matrix. Therefore, the construction of a constitutive SMPC model is complicated.

**5.1 Constitutive theories of Particle Reinforced Shape Memory Polymers Composites.** There are several effective models for predicting the thermodynamic properties of particulate-reinforced SMPCs. The most common modeling method is the conventional viscoelastic method combined with the micromechanics theory, including the self-consistent theory [84–88] and Mori–Tanaka method [89]. Combined with the Mori–Tanaka theory, Yang et al. [90] investigated the mechanical properties of SMPCs based on the assumption of a uniform distribution of the particle phase. The changes in the mechanical properties of SMPCs with temperature and volume fraction of the inclusion phase were systematically investigated. Xu et al. [91,92] investigated a type of SMPC foam consisting of styrene-based SMPs and deformable glass microspheres using a combined rheology and phase transition model.

Baghani et al. [93] developed a model to investigate the mechanical properties of particulate-reinforced SMPCs under different loading conditions. The SMPCs were divided into two parts: the SMP and the hard segment. The SMPs were further divided into glassy and rubbery phases (Fig. 13). The reinforced, glassy, and rubbery phases are considered viscoelastic materials. The strain satisfies the Clausius–Duhem inequality and is divided into six parts, including the SMP strain, $\varepsilon_p$; reinforcement phase strain, $\varepsilon_h$; irrecoverable strain, $\varepsilon_i$; and thermal strain, $\varepsilon_T$

$$\varepsilon = \phi_p \varepsilon_p + \phi_h \varepsilon_h + \varepsilon_i + \varepsilon_T \qquad (25)$$

where $c$ and $p$ denote the reinforcement phase and SMP matrix, respectively, and $\phi_p$ and $\phi_h$ the volume fractions of the SMP matrix and hard segment phase, respectively.

Velmurugan et al. [94] investigated the influence of microstructure parameters and strain rate on multiwalled carbon nanotubes/SMPCs. Jarali et al. [95] extended the single inclusion theory to the double inclusion problem by employing Eshelby's model. By investigating the interaction between the matrix and inclusion phase (carbon fiber and carbon nano tube), the effective mechanical properties of SMPCs were obtained, and analytical solutions under low-strain deformations were derived. Taherzadeh et al. [96] proposed a constitutive model for particulate-reinforced SMPCs and analyzed it with finite element software. By establishing representative volume elements, the author investigated the mechanical properties of SMPCs with different nanoparticle volume fractions and length–width ratios.
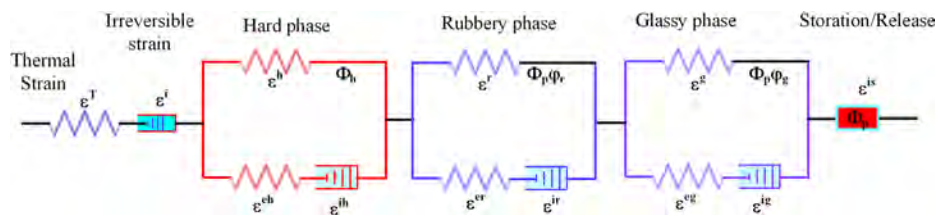


**Fig. 13 Schematic of the constitutive model proposed by Baghani et al.**

Based on the assumption of homogeneous isotropy, Yin et al. [97] developed a modified viscoelastic constitutive theory and investigated the thermodynamic properties and shape-recovery behavior of particulate-reinforced SMPCs. The model combined the modified Adams–Gibbs and Eyring models to describe the relaxation and yield behavior and employed the non-Gaussian molecular network model to characterize the hyperelastic properties under significant deformations (Table 4a). The free recovery behavior of SMPCs with different particle fractions and the stress–strain response with temperature were estimated. The temperature-dependent modulus of SMPCs was considered as a combination of the additional Prony chain and pure SMP matrix systems

$$E(T) = E_0 + E_1 \exp\left[-\left(\frac{T}{T_1}\right)^{\beta_1}\right] + E_2 \exp\left[-\left(\frac{T}{T_2}\right)^{\beta_2}\right]$$
$$+ E_3 \exp\left[-\left(\frac{T}{T_3}\right)^{\beta_3}\right] \quad (26)$$

where $E_0$ denotes the equilibrium modulus, $E_1$ and $E_2$ the reference moduli, $\beta_1$ and $\beta_2$ the Prony parameters, and $E_3$ and $\beta_3$ the parameters related to the inclusion phase.

Combined with the micromechanical model and network transition theory, Zeng et al. [98] investigated the effective mechanical properties, potential mechanisms of stress relaxation, and shape memory behavior of SMPCs. This study assumed that the SMPCs were composed of a backbone and transient networks (Table 4b). Employing the thermal viscoelastic–hyperelastic constitutive model and Monte Carlo algorithm network, Yarali et al. [99] proposed a representative volume element of SMPCs and investigated the homogenization of helical carbon-nanotube-reinforced SMPCs under high deformation conditions. In this study, a hyperelastic model was introduced into the model to describe the stress of the elastic part, and Maxwell–Wiechert components were employed to describe the viscoelastic part (Table 4c). Using the finite element method, the shape recovery properties of SMPCs under different heating rates and prestrains were investigated. Furthermore, the author explored the effect of the volume fraction on the SMPC properties, orientation, and geometric parameters of reinforcement. Subsequently, Zeng et al. [100] established a micromechanical theory and characterized the mechanical properties of SMPCs combined with the Mori–Tanaka method (Table 4d).

Combined with GMM, Zhao et al. [101] established a viscoelastic constitutive relationship of particulate-reinforced SMPs using the Mori–Tanaka method. Through Laplace transformation, the viscoelastic response of the model was linear in the Laplace domain. Hence, the author predicted the thermal–mechanical cycle process of SMPCs and explored the variation law of the elastic modulus with temperature and inclusion volume fractions.

### 5.2 Constitutive Theory of Fiber-Reinforced Shape Memory Polymers Composites.
Nishikawa et al. [102] investigated the mechanical behavior of short-fiber-reinforced SMPCs using the finite element method. The model developed by Tobushi et al. [13] was employed to describe the mechanical behavior of the SMP matrix, whereas the carbon fiber phase was represented by an orthotropic elastomer. However, the simulated results indicate that the local irrecoverable deformation becomes significant owing to the addition of short carbon fibers. Furthermore, even though the overall strain of the material was set at 8%, owing to the stress concentration effect, the strain in the local areas reached 15%. Furthermore, irrecoverable deformation affects the shape-recovery effect. Consequently, only by establishing a model that considers the microstructure of the fiber and SMP and investigating the local strain concentration effect, can the SME and quantitative calculation of the irrecoverable strain be accurately

determined. Masaaki et al. [103] developed a periodic unit method and investigated the effects of fiber content and geometrical parameters on the mechanical properties of SMPCs.

Based on the phenomenological theory framework, Ge et al. [104] developed a constitutive model for fiber-reinforced SMPCs. In this study, SMPs and fibers were regarded as heterogeneous solids, in which the fiber was assumed to be a complex solid, and the SMPs were assumed to be a composite elastomer with melt and crystalline phases. The multibranch model on the right represents the crystallization process of the matrix at different times. When the matrix phase crystallizes, the switch opens, and the material can carry the load. When the material is in the molten state, the switch closes, and the material cannot carry the load (Table 4e).

The departure of the stress distribution in SMPCs was described by the micromechanics of heterogeneous solids. By dividing SMPCs into a rubbery phase, glassy phase, and fiber reinforcement, Tan et al. [105] established a fiber-reinforced SMPC constitutive model combined with the bridging model and phase evolution theory. The bridging model assumes that the matrix and fiber surfaces are closely connected before the failure of the composite. The internal stress, $\sigma_i^m$, in the matrix, and $\sigma_i^f$ in the fiber are connected by a nonsingular matrix $[A_{ij}]$. This model qualitatively analyzed the influences of the ambient temperature and fiber volume fraction on the SME and recovery force. However, this model does not consider the anisotropy of the fiber, the interaction between the fiber and matrix, or thermal residual stress between the fiber and matrix. The key equations involved in this model are as follows:

$$\begin{cases} \varepsilon_i = \varepsilon_i^f \psi_f + \varepsilon_i^g \psi_g + \varepsilon_i^r \psi_r + \varepsilon_T + \varepsilon_n^{gs} \\ \sigma_i = \sigma_i^T + \sigma_i^{rec} + \sigma_i^C \\ \sigma_i^C = \psi_f \sigma_i^f + \psi_g \sigma_i^g + \psi_r \sigma_i^r \\ \sigma_i^m = \phi_g \sigma_i^g + \phi_r \sigma_i^r \\ \sigma_i^m = [A_{ij}](\psi_f \delta_{jk} + \psi_m [A_{jk}])^{-1} \sigma_k = [A_{ij}][B_{jk}]\sigma_k \end{cases} \quad (27)$$

where $g$, $r$, and $f$ denote the glassy phase, rubbery phase, and fibers, respectively. $\varepsilon_T$ denotes the thermal strain, and $\varepsilon_n^{gs}$ the storage and release of strain during heating and cooling. $\psi_f$ denotes the volume fraction of the fibers.

The deformations of woven fabric-reinforced SMPCs (WF-SMPCs) are complex because temperature changes result in thermal stress and significantly affect the interaction between the matrix and fibers. Roh et al. [106] investigated the time-dependent viscoelastic and unfolding behavior of thin-walled SMPC cantilever beams through experiments and numerical analyses and derived the viscoelastic constitutive model of SMPCs. The constitutive model was established by considering the interaction between the fabric and SMP matrix. The mechanical behavior of SMPs is described by a phenomenological model, that is, the SMP is composed of glassy and rubbery phases. The stress–strain relationships of the rubbery and glassy phases are described by multichain models (Table 4f). The overall deformation of the SMP matrix includes thermal, elastic, and storage strains. Employing this model, the shape recovery and viscoelastic properties of WF-SMPCs under high temperatures were investigated, providing a theoretical basis for its application in deployable structures.

Su et al. [107,108] established an anisotropic viscoelastic constitutive model for WF-SMPCs. The anisotropic hyperelastic mechanical behavior of woven fabrics is represented by spring elements, whereas the isotropic viscoelastic mechanical behavior is represented by the generalized Maxwell model. It was assumed that the deformations of the woven fabric and matrix were the same during the thermodynamic loading process. Because the mechanical strength of the matrix changes with temperature, the mechanical contribution of the fabric to the composite is different in the shape memory cycles. A temperature correction

coefficient, $C_f(T)$, was introduced to correct the contribution of the fabric to the total Helmholtz free energy. The second Piola–Kirchhoff stress, $S$, can be expressed as

$$\psi = \psi_{\text{matrix}} + C_f(T)\psi_{\text{fabric}} + \psi_T \tag{28}$$

$$\mathbf{S} = \mathbf{S}_{\text{matrix}} + C_f\mathbf{S}_{\text{fabric}} \tag{29}$$

where $\psi_{\text{matrix}}$, $\psi_{\text{fabric}}$, and $\psi_T$ denote the Helmholtz free energies related to the matrix, fabric, and temperature, respectively, and $\mathbf{S}_{\text{matrix}}$ and $\mathbf{S}_{\text{fabric}}$ denote the second Piola–Kirchhoff stresses of the matrix and fabric, respectively.

Short fiber-reinforced SMPCs exhibit better mechanical properties than pure SMPs while maintaining a high deformation capacity and excellent shape memory performance. Based on the temperature-dependent laminate theory, Zeng et al. [109] proposed a viscoelastic model for short fiber-reinforced-SMPCs and investigated the thermodynamic behavior of SMPCs under different loads. This model was modified based on the SLS model shown in Table 4g, in which the yield characteristics were related to the fiber content and represented by the modified Erying model.

Gu et al. [110] developed a thermodynamic coupling model for SMPCs based on the isotropic hypothesis using the internal variable method. The deformation was divided into three parts: thermal, hyperelastic, and viscoelastic deformations. The mechanical deformation of SMPCs can be divided into elastic equilibrium and viscoelastic nonequilibrium parts related to the time response. The stress of the mechanical deformation part, $\boldsymbol{\sigma}^m$, was divided into $\boldsymbol{\sigma}^n$ and $\boldsymbol{\sigma}^v$ because the dashpot element and spring in the nonequilibrium part are connected in series, and their stresses are equal. Therefore, $\boldsymbol{\sigma}^m$ can be further divided into the stress in the equilibrium part, $\boldsymbol{\sigma}^n$, and the stress of the spring in the nonequilibrium part, $\boldsymbol{\sigma}^e$. Notably, the equilibrium part stress, $\boldsymbol{\sigma}^n$, is expressed as fiber-reinforced transversely isotropic hyperelastic composites, proposed by Guo et al. [111].

Furthermore, the viscoelastic part was divided into the equilibrium and nonequilibrium parts related to time. The thermal deformation was described using the two-phase homogenization theory. The key equations involved in the model can be expressed as

$$\boldsymbol{\sigma}^m = \boldsymbol{\sigma}^n + \boldsymbol{\sigma}^e$$
$$\boldsymbol{\sigma}^n = -p\mathbf{I} + G_e\,\mathbf{F}^m(\mathbf{F}^m)^{\text{T}} + cG_c\left(1 - \mathbf{I}_4^{-2/3}\right)\mathbf{F}^m\boldsymbol{a}_0 \otimes \mathbf{F}^m\boldsymbol{a}_0 \tag{30}$$
$$\boldsymbol{\sigma}^v = \boldsymbol{\sigma}^e = \frac{1}{J^e}\mathbf{L}^e : \mathbf{E}^e$$

where $\mathbf{I}$ denotes the second-order unit tensor, $p$ the hydrostatic pressure, $\mathbf{F}^m$ the deformation gradient of the mechanical part, $G_c$ the effective shear modulus of the SMPC, $\mathbf{I}_4 = \boldsymbol{a}_0 \cdot \mathbf{C}^m \cdot \boldsymbol{a}_0$, $\mathbf{C}^m = \mathbf{F}^{m\text{T}}\mathbf{F}^m$, $\boldsymbol{a}_0$ the fiber direction in the initial configuration, and $c$ the material parameter.

However, this model did not consider the anisotropy of SMPCs, the different thermal expansion properties below and above the $T_g$, or the interaction between the matrix and fibers. Furthermore, the residual stresses caused by the differences in the elastic modulus and thermal expansion between the matrix and fibers were not involved.

Currently, there are several constitutive studies on the anisotropy of unidirectional and braided reinforced composites. The theory proposed by Peng et al. [112], which has physical significance, is typically used for anisotropic composites. Hong et al. [113] divided the energy of the SMPC into the matrix, fiber tensile, and fiber shear energies, and deduced the stress expression of the SMPC while investigating the WF-SMPCs. The theory developed by Park et al. [79] was employed to describe the mechanical properties of an SMP matrix. As shown in Table 4h, the SMP matrix consists of the active and frozen phases. $r$ and $g$ denote the active and frozen phases, and $e$, $v$, $p$, and $nm$ represent the elastic,

viscous, plastic, and shape memory strains, respectively. The model considered the anisotropy of the SMPCs and described the residual thermal stress using Eshelby's equivalent inclusion model. The average thermal residual stress in the SMPC was calculated using the intrinsic strain and stress distributions in the cylindrical space.

Table 4 summarizes the schematics of the constitutive models of the SMPCs mentioned above.
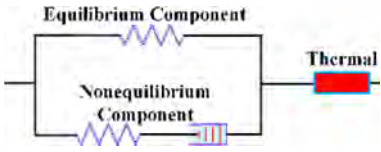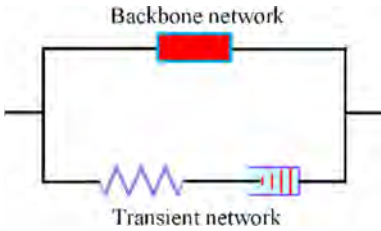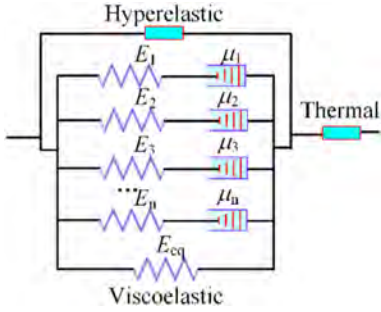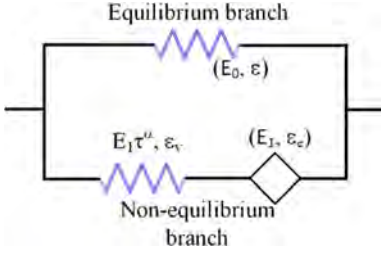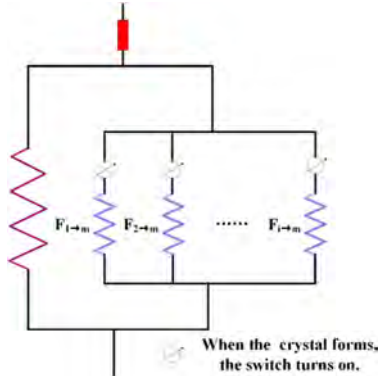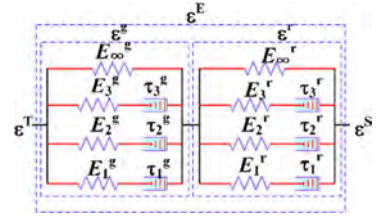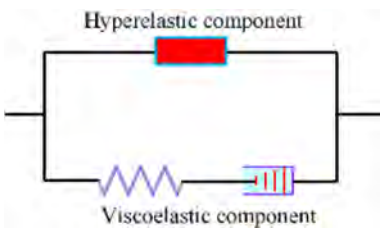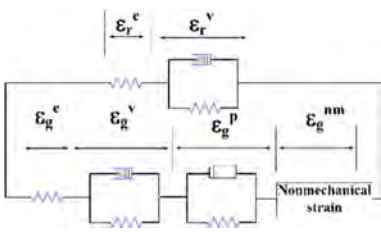
### 5.3 Buckling and Post-Buckling Behavior of Shape Memory Polymers Composites.

Continuous fiber-reinforced SMPCs (CF-SMPCs) exhibit advantages such as high specific stiffness and strength, simple formation, and low density. In addition, CF-SMPCs exhibit a significant folding deformation at high temperatures and have been widely employed in space deployable structures. By folding the structure, the loading space and launch cost can be effectively decreased. When transported to a specified orbit, the structure can recover its initial shape by heating it to a temperature above its $T_g$. During folding, the SMPC exhibits a geometrical nonlinearity deformation similar to that of the strip spring, and the fibers inside the SMPC undergo microbuckling deformation under compression (Fig. 14), changing the macroscopic stiffness of the structure.

A critical mechanical problem is the deformation of the fiber after reaching the critical buckling load. The maximum deformation ratio of conventional CF-SMPCs is determined by the fracture elongation of the fiber, which is typically less than 2%. However, because SMPCs are sensitive to temperature, their modulus at high temperatures is low (only a few MPa). The fiber can generate a significant buckling deformation without breaking by subjecting the SMPC to bending deformation at high temperatures. Microbuckling is the reason why SMPCs can withstand significant bending deformations. When the SMP matrix is softened at high temperatures, it does not have sufficient stiffness to support the compressed fiber, and the fiber undergoes microbuckling owing to the low shear modulus of the SMP. The material can maintain good mechanical and shape-memory properties under significant macroscopic bending deformations.

To investigate the buckling behavior of SMPCs, theoretical research methods such as homogenization, Bloch wave, and strain energy function methods have been employed. Some 3D constitutive models of fiber-reinforced flexible composites were developed combined with the second-order homogenization theory and employed the Neo-Hookean model to represent the response of the matrix [114,115]. Although this method has been improved, it is essentially a nonlinear theoretical problem, which is still difficult to solve accurately, and obtaining microscopic local stresses and strains is challenging [116–118]. The Bloch wave theory has some advantages in analyzing the deformation and damage evolution of laminated material microstructures. However, it requires complex programing and numerical computing capabilities, limiting its application in the deformation analysis of fiber-reinforced flexible composites [119]. Furthermore, according to the strain energy function, the total strain energy can be obtained by summing the tensile, compressive, and shear strain energies of the fiber and matrix. Hence, the fiber buckling half-wavelength, fiber buckling amplitude, neutral plane position, and macroscopic strain of the composite laminates can be obtained.

When SMPCs undergo a significant bending deformation, they produce microbuckling in the compression zone and affect the macrostiffness [120]. Timoshenko et al. [121] used an elastic matrix as a group of parallel spring elements to determine the strain energy. According to the total strain energy being equal to the work done by the external force, the authors determined the critical load of fiber buckling. Based on Timoshenko's study, Rosen et al. [122] developed a buckling model for unidirectional fiber-reinforced composites. The goal was a 2D simplified model of a unidirectional plate, which is equivalent to a fiber and matrix layer evenly interbedded. However, the results of tensile buckling

**Table 4  Summary of the schematics of constitutive models of SMPC**

| | Schematics | References | | Schematics | References |
|---|---|---|---|---|---|
| a | Equilibrium Component / Nonequilibrium Component / Thermal | [94] [97] | b | Backbone network / Transient network | [98] |
| c | Hyperelastic / $E_1, \mu_1$ / $E_2, \mu_2$ / $E_3, \mu_3$ / $\cdots E_n, \mu_n$ / $E_{eq}$ / Thermal / Viscoelastic | [99] | d | Equilibrium branch $(E_0, \varepsilon)$ / $E_1 \tau^\mu, \varepsilon_v$ $(E_1, \varepsilon_e)$ / Non-equilibrium branch | [100] |
| e | $F_{1\to m}$ $F_{2\to m}$ $\cdots\cdots$ $F_{i\to m}$ / When the crystal forms, the switch turns on. | [104] | f | $\varepsilon^E$ / $\varepsilon^g_g$ $\varepsilon^r$ / $E^g_\infty$ $E^r_{po}$ / $E^g_3 \tau^g_3$ $E^r_3 \tau^r_3$ / $E^g_2 \tau^g_2$ $E^r_2 \tau^r_2$ / $E^g_1 \tau^g_1$ $E^r_1 \tau^r_1$ / $\varepsilon^T$ $\varepsilon^S$ | [106] |
| g | Hyperelastic component / Viscoelastic component | [119] | h | $\varepsilon^e_r$ $\varepsilon^v_r$ / $\varepsilon^e_g$ $\varepsilon^v_g$ $\varepsilon^p_g$ $\varepsilon^{nm}_g$ / Nonmechanical strain | [113] |



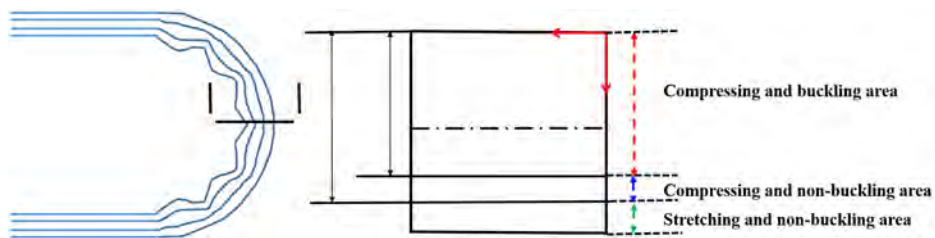**Fig. 14  Illustration of the bending deformation of fiber-reinforced SMPCs and strain state of the cross section**

Compressing and buckling area

Compressing and non-buckling area

Stretching and non-buckling area

are significantly different from those of the experimental observations, indicating the limitations of the model. According to this model, the minimum critical stress of the structure under shear and tensile buckling is calculated as follows:

$$\sigma_{cr}^{S} = \frac{\pi^2 E_f v_f h^2}{12\lambda^2} + \frac{G_m}{1 - v_f}, \quad \sigma_{cr}^{T} = \frac{\pi^2 E_f v_f h^2}{12} + \left[\frac{24\lambda^2 E_m}{\pi^4 ch^3 E_f} + \frac{1}{\lambda^2}\right]$$

(31)

where $\sigma_{cr}^{S}$ and $\sigma_{cr}^{T}$ denote the shear and tensile stresses, respectively; $\lambda$ the half-wavelength of the fiber buckling; $v_f$ the volume fraction of the fiber; $E_f$ and $E_m$ the elastic moduli of the fiber and matrix, respectively; $G_m$ the shear modulus of the matrix; and $h$ the diameter of the fiber.

Through preliminary theoretical studies and experimental observations, Gall [123] found that when composite laminates were folded along a cylinder with a certain curvature, the fiber inside the laminates deformed less owing to local buckling. However, the laminates maintained an excellent structural performance after deformation recovery. Composite Technology Development conducted extensive research on the buckling deformation of SMPCs, including mechanistic studies, experimental tests, and practical applications. It includes the observation of the failure strains, buckling mode of epoxy-based SMPCs, testing of the bending performance and finite element verification, and a study of the theoretical viscoelastic constitutive relation and failure mode [124–127]. Taking the neutral plane as the boundary, Francis et al. [127] established the strain energy equation of SMPCs by dividing the cross section into tensile and compression buckling regions. Based on this model, a solution was derived for the half-wavelength of the fiber microbuckling under bending deformation. However, the premise of the model was developed based on the assumption that microbuckling had already occurred, and the neutral layer coincided with the critical microbuckling layer. Consequently, the model cannot predict the slight deformation stage before microbuckling occurs and only applies to a situation of significant deflection.

Based on Timoshenko's study, Campbell et al. [128,129] further investigated the microbuckling behavior of the elastic matrix after embedding long fibers and proposed a theoretical model for the microbuckling of long-fiber SMPC plates. Based on the energy equation, the buckling half-wavelength can be expressed as follows:

$$\lambda_{cr} = \sqrt{\frac{\pi^4 E_f I_f}{3 G_m \left(\frac{d}{t}\right)^2}}$$

(32)

$$\varepsilon = \frac{1}{2L}\int_0^L \left(\sqrt{(dx)^2 + (dy)^2} - dx\right) dx \approx \frac{1}{2L}\int_0^L \left(\frac{dy}{dx}\right)^2 dx$$

where $I_f$ denotes the moment of inertia of the fiber section, and $t$ the thickness of the laminate.

Furthermore, Hutchinson, Suo, Huang, and Roger et al. [130–133] investigated the buckling problem of CF-SMPCs. These theoretical buckling models are based on pure tensile or shear modes. The experimental results indicated that shear buckling occurred mainly during the flexural loading of the laminates. However, owing to the different distribution locations of the fibers from the neutral layer, the nominal flexural strain of the fibers in different layers was different, resulting in a difference in the fiber buckling amplitude. Therefore, in addition to shear buckling, tensile buckling must be considered in the buckling model.

To analyze the post-buckling properties, Campbell et al. [134] assumed that SMPCs followed a double linear constitutive relationship. With the buckling surface layer as the boundary, the plates were divided into buckling and nonbuckling zones. The position coefficient of the neutral layer was deduced based on the resultant force of the cross section along the longitudinal direction to be zero under pure bending conditions. Because the

bending moment on the cross section was equal to the moment of the external force couple, they established a numerical analysis model of the SMPC. Francis [135] investigated the local post-buckling behavior of fibers during bending deformation and obtained key parameters, such as the offset distance where the neutral plane strain was zero and the fiber buckling wavelength.

Furthermore, Lake et al. [136] investigated the mechanical properties of SMPCs. The experimental results indicated that the buckling of the SMPC laminates always exhibited a sinusoidal shape. Wang et al. [137] proposed a unidirectional fiber-reinforced SMPC microbuckling model that can predict the buckling wavelength. The strain energy equations of the in-plane and out-of-plane bucklings were established, and the buckling was analyzed from two angles.

These theoretical buckling models were all proposed based on the assumption of pure tensile or shear modes; however, during the bending of laminates, the fiber undergoes mixed shear/tensile buckling deformations. Therefore, Wang et al. [138] proposed a simplified 2D tensile/shear coupling buckling model, where the critical buckling wavelength can be expressed as

$$\lambda_c = 2\pi^4 \sqrt{\frac{2 E_f I_f c}{E_m h} \cdot \frac{\sum_1^n \left(2i - 1 - 2\sqrt{i(i-1)}\right)}{n(n+1)}}$$

(33)

where $n$ denotes the laminate-fiber layer. The critical buckling wavelength obtained by this equation correlates well with the experimental observations; however, the model is established based on the 2D structure of the unidirectional fiber.

By dividing the flexural deformation of the fiber-reinforced SMPCs into three regions: compressing and buckling areas, compressing and nonbuckling areas, and stretching and nonbuckling areas, Lan et al. [120] developed an analysis model and obtained a strain energy expression. The amplitude of the buckling fibers and the position of critical buckling were obtained and calculated. It was theoretically verified that a significant macroscopic bending deformation can be obtained by slight buckling. The strain energy of CF-SMPCs during finite deflection was investigated using the thermodynamic energy method, and the critical buckling was obtained according to the minimum energy principle as follows:

$$k_c = \frac{4M}{t}$$

(34)

$$\lambda_{cr} = \begin{cases} +\infty & (k < k_c) \\ \left[\dfrac{8\pi^3 V_f E_f I_f \left(z_{ns}^2 - \dfrac{4M^2}{k^2}\right)^2}{V_m G_m h \ln\left(\dfrac{k z_{ns}}{2M}\right)}\right]^{0.25} & (k \geq k_c) \end{cases}$$

(35)

where $k$ is the curvature, and $M = V_m G_m / (V_m E_m + V_f E_f)$, and $z_{ns}$ represents the neutral plane.

Tan [139] developed a buckling model for metal film/fiber-reinforced SMPCs under significant deflections and provided an analytical expression of the key parameters of buckling deformation. The relationship between the recovery force, recovery moment of the SMPC laminates, and geometrical parameters of the structure were obtained using the model. The main energy forms of the composites during deformation were analyzed, and the total energy equation was calculated. Using the principle of minimum potential energy, the critical strain of the structure was obtained, and the fiber-buckling problem was analyzed using the finite element method. The critical strain can be expressed as

$$\varepsilon_{cr} = 4\frac{h}{f E_{xx}}\left(z - \left(1 + \frac{E_m t}{E_{xx}} - \frac{f}{h}(g + G_s v_s)\right)\right)$$

(36)

where $h$ and $f$ can be expressed as $h = v_s G_s (E_m t + E_{xx} z_m)$ and $f = E_{xx} z_m^2 + E_m t^2 + 2 E_m t z_m$, respectively.

The assumption that the matrix around the buckling fiber had a uniform shear strain in the 1D beam and 2D plane model affected the prediction of the local shear failure. Therefore, Zhang et al. [140] developed an analytical model by assuming a fiber to be a 3D solid and investigated the size effect on the shear strain. The solution of the half-wavelength changing with fiber content was determined by Francis et al. [135] and Lan et al. [120], and can be expressed as

$$\lambda = \left[ \frac{E_f v_f \pi^4 h^2 t^2}{8 G_m f(v_f) \left[ -1 + \ln\left( \frac{8t}{h} \sqrt{\frac{v_f}{\pi}} \right) \right]} \right]^{1/4} \quad (37)$$

## 6 Necessary Experimental Methods to Obtain Parameters

To characterize the mechanical properties and obtain the model parameters of SMPs and SMPCs, a series of dynamic and static mechanical property tests are often performed, including dynamic thermomechanical analysis, tensile tests, creep/stress relaxation tests, and high- and low-temperature recovery tests. Because the mechanical properties of SMPs and SMPCs are closely related to the temperature, variable temperature experiments are often performed. In addition, because the most useful property of this type of material is shape memory, the thermal–mechanical cycle experiment is a basic experiment.

(1) Static mechanical property tests
Static mechanical property tests are the main methods used to study the mechanical properties of SMPs and SMPCs. According to the different test requirements, two test modes are typically employed: stretching and three-point bending. Because the mechanical properties of SMPs and SMPCs vary significantly before and after the glass transition, and the material parameters, such as elastic modulus, change significantly, the environmental temperature of mechanical experiments is typically involved before and after the glass transition. Uniaxial tensile experiments were performed at different temperatures and constant strain rates to determine the variations in the elastic modulus, yield strain, yield stress, ultimate strain, and ultimate stress of SMPs and SMPCs with temperature.

(2) Differential scanning calorimetry
Differential scanning calorimetry is an important thermal analysis method that can effectively measure the phase transition and glass transition behaviors of materials. The change in mechanical properties, such as the transition from the highly elastic to glassy states, of the sample during temperature change changes the specific heat, which is reflected as the "jitter" of the baseline in the experimental curve. During DSC experiments, the samples undergo phase and glass transitions, accompanied by clear heat absorption and exothermic phenomena. This method mainly determines the glass transition behavior of SMPs and obtains the glass transition temperature.

(3) Dynamic thermomechanical analysis
Dynamic mechanical analysis is primarily used to measure the mechanical properties of viscoelastic materials, which change with time, temperature, and frequency. Owing to the viscoelastic properties of polymer materials, there is a significant delay between the mechanical response strain (stress) and applied high-frequency stress (strain). The variation law of material parameters, such as the energy storage modulus, loss modulus, and loss angle with temperature, can be obtained by measuring the relationship between the high-frequency external excitation and material response. This method mainly determines the dynamic mechanical properties of the $T_g$, loss modulus, and loss angle.

(4) Shape-recovery ratio
The shape-recovery properties of SMPs and SMPCs are an important issue in studies on this type of material. The recovery characteristics of SMPs and SMPCs are significantly affected by the ambient temperature, and the recovery ratios of SMPs and SMPCs differ under different temperature conditions. At low temperatures, the molecular micro-Brownian motion is poor, and the pre-strain cannot be fully recovered after unloading, resulting in a residual strain. With an increase in temperature, the recovery characteristics gradually improve. Under high-temperature conditions, the micro-Brownian motion improves significantly. In the absence of an external load, the stretched molecular chain can rapidly return to its initial shape, which is macroscopically reflected in excellent shape-memory characteristics.

(5) Viscoelastic–mechanical properties
Creep and stress relaxation are important viscoelastic properties of SMPs and SMPCs. The study of viscoelastic properties is significant for accurately characterizing mechanical behavior. Creep and stress relaxation experiments were performed at different temperatures to determine the variations in delay time, relaxation time, and creep compliance with temperature.

## 7 Summary and Outlook

With the increasing studies on SMPs and their composites, several SMPs and SMPCs have emerged, and their applications have developed rapidly. Owing to the wide variety of SMPs, complex mechanisms, and different operating conditions, more applicable and high-precision constitutive models are still being developed. Moreover, there are only a few theoretical models that can describe the internal shape memory mechanisms of semicrystalline, optical actuation, and solution actuation SMPs, and must be considered.

Phase transition models are established based on the SME of SMPs and have fewer parameters than the viscoelastic model. Rheological models are developed based on time-dependent thermodynamic properties; therefore, they have more advantages in terms of universality. Combining the two modeling methods, the constitutive models have a clearer physical meaning and can better describe the shape memory mechanism. Consequently, the modeling of SMPs and SMPCs should develop toward a direction with more explicit physical meaning and general form, facilitating the development and design of new types of SMPs, SMPCs, and structural systems. Furthermore, establishing a generalized model with fewer parameters is a possibility for future studies.

For the buckling analysis of SMPCs, the expression of deformation energy was obtained by deformation analyses. Critical parameters, such as the critical bending moment, strain, and wavelength, can be determined according to the minimum potential energy. However, most theoretical analyses have mainly focused on the folding deformation of unidirectional materials, and the correlation analysis for WF-SMPCs is lacking. Furthermore, the analysis of the interaction between the fiber and matrix and the residual stress of the matrix and fiber are the main directions for future SMPC constitutive models.

## Conclusions

The constitutive models of SMPs can be divided into rheological and phenomenological models, as well as a combination of the two models. The rheological model of SMPs can be represented by different combinations of the spring and dashpot elements. Studies have modified the model by introducing nonlinear terms,

rate- and temperature-dependent terms, and multiple branches to describe the more complex viscoelastic behavior of SMPs. However, this type of model typically contains a significant number of parameters and cannot reasonably describe the storage and release of strain. Phenomenological models can clearly describe the freezing and release of strain in the thermodynamic cycle, but they cannot describe the viscoelastic behavior. Combining the rheological method at the macroscopic scale with the phenomenological method at the molecular level is an effective solution. Compared to SMPs, theoretical studies on the mechanical properties of SMPCs are limited. Except for a few specific SMPC structures, such as beams and plates, the predictability of the constitutive model is limited, particularly for dynamic performance. As the range of SMPC-based applications expands, it is necessary to establish relevant theoretical models to study mechanical behavior in-depth and provide a theoretical basis for its future applications.

## Funding Data

## References

[1] Zhao, W., Liu, L. W., Zhang, F. H., Leng, J. S., and Liu, Y. J., 2019, "Shape Memory Polymers and Their Composites in Biomedical Applications," Mat. Sci. Eng. C-Mater., 97, pp. 864–883.

[2] Zhao, W., Yue, C. B., Liu, L. W., Leng, J. S., and Liu Y. J., 2023, "Mechanical Behavior Analyses of 4D Printed Metamaterials Structures With Excellent Energy Absorption Ability," Compos. Struct., 304, p. 116360.

[3] Zhao, W., Zhang, F. H., Leng, J. S., and Liu, Y. J., 2019, "Personalized 4D Printing of Bioinspired Tracheal Scaffold Concept Based on Magnetic Stimulated Shape Memory Composites," Compos. Sci. Technol., 184, p. 107866.

[4] Zhao, W., Huang, Z. P., Liu, L. W., Wang, W. B., Leng, J. S., and Liu, Y. J., 2021, "Porous Bone Tissue Scaffold Concept Based on Shape Memory PLA/Fe₃O₄," Compos. Sci. Technol., 203, p. 108563.

[5] Urbina, L., Alonso-Varona, A., Saralegi, A., Palomares, T., Eceiza, A., Corcuera, M., and Retegi, A., 2019, "Hybrid and Biocompatible Cellulose/Polyurethane Nanocomposites With Water-Activated Shape Memory Properties," Carbohyd. Polym., 216(15), pp. 86–96.

[6] Zhao, W., Li, N., Liu, L. W., Leng, J. S., and Liu, Y. J., 2022, "Origami Derived Self-Assembly Stents Fabricated via 4D Printing," Compos. Struct., 293, p. 115669.

[7] Zhao, W., Huang, Z. P., Liu, L. W., Wang, W. B., Leng, J. S., and Liu, Y. J., 2022, "Bionic Design and Performance Research of Tracheal Stent Based on Shape Memory Polycaprolactone," Compos. Sci. Technol., 229, p. 109671.

[8] Wang, F., Yuan, C., Wang, D., Rosen, D. W., and Ge, Q., 2020, "A Phase Evolution Based Constitutive Model for Shape Memory Polymer and Its Application in 4D Printing," Smart Mater. Struct., 29(5), p. 055016.

[9] Mao, Y., Chen, F., Hou, S., Qi, J., and Yu, K., 2019, "A Viscoelastic Model for Hydrothermally Activated Malleable Covalent Network Polymer and Its Application in Shape Memory Analysis," J. Mech. Phys. Solids, 127, pp. 239–265.

[10] Wang, X., Lu, H. B., Shi, X., Yu, K., and Fu, Y. Q., 2019, "A Thermomechanical Model of Multi-Shape Memory Effect for Amorphous Polymer With Tunable Segment Compositions," Compos. Part B-Eng., 160, pp. 298–305.

[11] Tobushi, H., Hashimoto, T., Hayashi, S., and Yamada, E., 1997, "Thermomechanical Constitutive Modeling in Shape Memory Polymer of Polyurethane Series," J. Intel. Mat. Syst. Str., 8(8), pp. 711–718.

[12] Lin, J., and Chen, L., 1999, "Shape-Memorized Crosslinked Estertype Polyurethane and Its Mechanical Viscoelastic Model," J. Appl. Polym. Sci., 73(7), pp. 1305–1319.

[13] Tobushi, H., Okumura, K., Hayashi, S., and Ito, N., 2001, "Thermomechanical Constitutive Model of Shape Memory Polymer," Mech. Mater., 33(10), pp. 545–554.

[14] Abrahamson, E. R., Lake, M. S., Munshi, N. A., and Gall, K., 2003, "Shape Memory Mechanics of an Elastic Memory Composite Resin," J. Intel. Mat. Syst. Str., 14(10), pp. 623–632.

[15] Morshedian, J., Khonakdar, H. A., and Rasouli, S., 2005, "Modeling of Shape Memory Induction and Recovery in Heat Shrinkable Polymers," Macromol. Theor. Simul., 14(7), pp. 428–434.

[16] Khonakdar, H. A., Jafari, S. H., Rasoul, S., Morshedian, J., and Abedini, H., 2007, "Investigation and Modeling of Temperature Dependence Recovery Behavior of Shape Memory Crosslinked Polyethylene," Macromol. Theor. Simul., 16(1), pp. 43–52.

[17] Bonner, M., Oca, H. M. D., Brown, M., and Ward, I. M., 2010, "A Novel Approach to Predict the Recovery Time of Shape Memory Polymers," Polymers, 51(6), pp. 1432–1436.

[18] Heuchel, M., Cui, J., Kratz, K., Kosmella, H., and Lendlein, A., 2010, "Relaxation Based Modeling of Tunable Shape Recovery Kinetics Observed Under Isothermal Conditions for Amorphous Shape-Memory Polymers," Polymers, 51(26), pp. 6212–6218.

[19] Li, Y. X., Guo, S. S., He, Y. H., and Liu, Z. S., 2015, "A Simplified Constitutive Model for Predicting Shape Memory Polymers Deformation Behavior," Int. J. Comput. Mat. Sci., 04(1), p. 1550001.

[20] Diani, J., Liu, Y., and Gall, K., 2006, "Finite Strain 3D Thermoviscoelastic Constitutive Model for Shape Memory Polymers," Polym. Eng. Sci., 46(4), pp. 486–492.

[21] Wong, Y. S., Stachurski, Z., and Venkatraman, S., 2011, "Modeling Shape Memory Effect in Uncrosslinked Amorphous Biodegradable Polymer," Polymers, 52(3), pp. 874–880.

[22] Ghosh, P., and Srinivasa, A. R., 2011, "A Two-Network Thermomechanical Model of a Shape Memory Polymer," Int. J. Eng. Sci., 49(9), pp. 823–838.

[23] Ghosh, P., and Srinivasa, A. R., 2013, "A Two-Network Thermomechanical Model and Parametric Study of the Response of Shape Memory Polymers," Mech. Mater., 60, pp. 1–17.

[24] Ghosh, P., and Srinivasa, A. R., 2014, "Development of a Finite Strain Two Network Model for Shape Memory Polymers Using QR Decomposition," Int. J. Eng. Sci., 81, pp. 177–191.

[25] Balogun, O. A., and Mo, C., 2014, "Shape Memory Polymers: Three-Dimensional Isotropic Modeling," Smart Mater. Struct., 23(4), p. 045008.

[26] Olaniyi, A., Balogun, and Changki, M., 2016, "Three-Dimensional Thermo-Mechanical Viscoelastic Model for Shape Memory Polymers With Binding Factor," J. Intel. Mat. Syst. Str., 27(14), pp. 1908–1916.

[27] Chen, J. G., Liu, L. W., Liu, Y. J., and Leng, J. S., 2014, "Thermoviscoelastic Shape Memory Behavior for Epoxy-Shape Memory Polymer," Smart Mater. Struct., 23(5), p. 055025.

[28] Nguyen, T. D., Qi, H. J., Castro, F., and Long, K. N., 2008, "A Thermoviscoelastic Model for Amorphous Shape Memory Polymers: Incorporating Structural and Stress Relaxation," J. Mech. Phys. Solids, 56(9), pp. 2792–2814.

[29] Xiao, R., Choi, J., Lakhera, N., Yakacki, C. M., Frick, C. P., and Nguyen, T. D., 2013, "Modeling the Glass Transition of Amorphous Networks for Shape-Memory Behavior," J. Mech. Phys. Solids, 61(7), pp. 1612–1635.

[30] Buckley, C. P., Prisacariu, C., and Caraculacu, A., 2007, "Novel Triol-Crosslinked Polyurethanes and Their Thermorheological Characterization as Shape-Memory Materials," Polymers, 48(5), pp. 1388–1396.

[31] Diani, J., Gilormini, P., Fredy, C., and Rousseau, I., 2012, "Predicting Thermal Shape Memory of Crosslinked Polymer Networks From Linear Viscoelasticity," Int. J. Solids Struct., 49(5), pp. 793–799.

[32] Arrieta, S., Diani, J., and Gilormini, P., 2014, "Experimental Characterization and Thermoviscoelastic Modeling of Strain and Stress Recoveries of an Amorphous Polymer Network," Mech. Mater., 68, pp. 95–103.

[33] Anand, L., Ames, N. M., Srivastava, V., and Chester., and S. A., 2009, "A Thermo-Mechanically-Coupled Theory for Large Deformations of Amorphous Polymers. Part I: Formulation," Int. J. Plast., 25(8), pp. 1474–1494.

[34] Ames, N. M., Srivastava, V., Chester, S. A., and Anand, L., 2009, "A Thermo-Mechanically-Coupled Theory for Large Deformations of Amorphous Polymers. Part II: Applications," Int. J. Plast., 25(8), pp. 1495–1539.

[35] Srivastava, V., Chester, S. A., Ames, N. M., and Anand, L., 2010, "A Thermo-Mechanically-Coupled Large-Deformation Theory for Amorphous Polymers in a Temperature Range Which Spans Their Glass Transition," Int. J. Plast., 26(8), pp. 1138–1182.

[36] Srivastava, V., Chester, S. A., and Anand, L., 2010, "Thermally Actuated Shape-Memory Polymers: Experiments, Theory, and Numerical Simulations," J. Mech. Phys. Solids, 58(8), pp. 1100–1124.

[37] Li, G. Q., and Xu, W., 2011, "Thermomechanical Behavior of Thermoset Shape Memory Polymer Programmed by Cold-Compression: Testing and Constitutive Modeling," J. Mech. Phys. Solids, 59(6), pp. 1231–1250.

[38] Westbrook, K. K., Kao, P. H., Castro, F., Ding, Y. F., and Qi, H. J., 2011, "A 3D Finite Deformation Constitutive Model for Amorphous Shape Memory Polymers: A Multi-Branch Modeling Approach for Nonequilibrium Relaxation Processes," Mech. Mater., 43(12), pp. 853–869.

[39] Yu, K., Xie, T., Leng, J. S., Ding, Y. F., and Qi, H. J., 2012, "Mechanisms of Multi-Shape Memory Effects and Associated Energy Release in Shape Memory Polymers," Soft Matter, 8(20), pp. 5687–5695.

[40] Yu, K., McClung, A. J. W., Tandon, G. P., Baur, J. W., and Qi, H. J., 2014, "A Thermomechanical Constitutive Model for an Epoxy Based Shape Memory Polymer and Its Parameter Identifications," Mech. Time-Depend. Mater., 18(2), pp. 453–474.

[41] Yu, K., Li, H., McClung, A. J. W., Tandon, G. P., Baur, J. W., and Qi, H. J., 2016, "Cyclic Behaviors of Amorphous Shape Memory Polymers," Soft Matter., 12(13), pp. 3234–3245.

[42] Sweeney, J., Bonner, M., and Ward, I. M., 2014, "Modelling of Loading, Stress Relaxation and Stress Recovery in a Shape Memory Polymer," J. Mech. Behav. Biomed., 37, pp. 12–23.

[43] Ge, Q., Yu, K., Ding, Y. F., and Qi, H. J., 2012, "Prediction of Temperature-Dependent Free Recovery Behaviors of Amorphous Shape Memory Polymers," Soft Matter, 2012 8(43), pp. 11098–11105.

[44] Gu, J. P., Sun, H. Y., and Fang, C. Q., 2015, "A Multi-Branch Finite Deformation Constitutive Model for a Shape Memory Polymer Based Syntactic Foam," Smart Mater. Struct., 24(2), p. 025011.

[45] Nguyen, T. D., Yakacki, C. M., Brahmbhatt, P. D., and Chambers, M. L., 2010, "Modeling the Relaxation Mechanisms of Amorphous Shape Memory Polymers," Adv. Mater., **22**(31), pp. 3411–3423.

[46] Fang, C. Q., Sun, H. Y., and Gu, J. P., 2016, "A Fractional Calculus Approach to the Prediction of Free Recovery Behaviors of Amorphous Shape Memory Polymers," J. Mech., **32**(1), pp. 11–17.

[47] Li, Z., Wang, H., Xiao, R., and Yang, S., 2017, "A Variable-Order Fractional Differential Equation Model of Shape Memory Polymers," Chaos. Soliton. Fract., **102**, pp. 473–485.

[48] Pan, Z., and Liu, Z., 2018, "A Novel Fractional Viscoelastic Constitutive Model for Shape Memory Polymers," J. Polym. Sci. Pol. Phys., **56**(16), pp. 1125–1134.

[49] Zeng, H., Leng, J., Gu, J., Yin, C., and Sun, H., 2018, "Modeling the Strain Rate-, Hold Time-, and Temperature-Dependent Cyclic Behaviors of Amorphous Shape Memory Polymers," Smart Mater. Struct., **27**(7), p. 075050.

[50] Zeng, H., Xie, Z. M., Gu, J. P., and Sun, H. Y., 2018, "A 1D Thermomechanical Network Transition Constitutive Model Coupled With Multiple Structural Relaxation for Shape Memory Polymers," Smart Mater. Struct., **27**(3), p. 035024.

[51] Liu, Y., Gall, K., Dunn, M. L., Greenberg, A. R., and Diani, J., 2006, "Thermomechanics of Shape Memory Polymers: Uniaxial Experiments and Constitutive Modeling," Int. J. Plast., **22**(2), pp. 279–313.

[52] Chen, Y. C., and Lagoudas, D. C., 2008, "A Constitutive Theory for Shape Memory Polymers. Part I: Large Deformations," J. Mech. Phys. Solids, **56**(5), pp. 1752–1765.

[53] Chen, Y. C., and Lagoudas, D. C., 2008, "A Constitutive Theory for Shape Memory Polymers. Part II: A Linearized Model for Small Deformations," J. Mech. Phys. Solids, **56**(5), pp. 1766–1778.

[54] Pan, Z., Zhou, Y., Zhang, N., and Liu, Z. S., 2018, "A Modified Phase Based Constitutive Model for Shape Memory Polymers," Polym. Int., **67**(12), pp. 1677–1683.

[55] Barot, G., and Rao, I., 2006, "Constitutive Modeling of the Mechanics Associated With Crystallizable Shape Memory Polymers," J. Z. Angew. Math. Phys., **57**(4), pp. 652–681.

[56] Barot, G., Rao, I. J., and Rajagopal, K. R., 2008, "A Thermodynamic Framework for the Modeling of Crystallizable Shape Memory Polymers," Int. J. Eng. Sci., **46**(4), pp. 325–351.

[57] Volk, B. L., Lagoudas, D. C., and Maitland, D. J., 2011, "Characterizing and Modeling the Free Recovery and Constrained Recovery Behavior of a Polyurethane Shape Memory Polymer," Smart Mater. Struct., **20**(9), p. 094004.

[58] Volk, B. L., Lagoudas, D. C., Chen, Y. C., and Whitley, K. S., 2010, "Analysis of the Finite Deformation Response of Shape Memory Polymers: I. Thermomechanical Characterization," Smart Mater. Struct., **19**(7), p. 075005.

[59] Volk, B. L., Lagoudas, D. C., and Chen, Y. C., 2010, "Analysis of the Finite Deformation Response of Shape Memory Polymers: II. 1D Calibration and Numerical Implementation of a Finite Deformation, Thermoelastic Model," Smart Mater. Struct., **19**(7), p. 075006.

[60] Volk, B. L., Dapino, M. J., Lagoudas, D. C., Ounaies, Z., and Chen, Y. C., 2008, "Thermomechanical Characterization of the Nonlinear Rate-Dependent Response of Shape Memory Polymers," Behav. Mech. Multifun. Compos. Mater., **6929**, pp. 261–269.

[61] Qi, H. J., Nguyen, T. D., Castro, F., Yakacki, C. M., and Shandas, R., 2008, "Finite Deformation Thermo-Mechanical Behavior of Thermally Induced Shape Memory Polymers," J. Mech. Phys. Solids, **56**(5), pp. 1730–1751.

[62] Gilormini, P., and Diani, J., 2012, "On Modeling Shape Memory Polymers as Thermoelastic Two-Phase Composite Materials," C. R. Mec., **340**(4–5), pp. 338–348.

[63] Kazakevičiūtė-Makovska, R., Steeb, H., and Aydin, A. Ö., 2012, "On the Evolution Law for the Frozen Fraction in Linear Theories of Shape Memory Polymers," Arch. Appl. Mech., **82**(8), pp. 1103–1115.

[64] Baghani, M., Naghdabadi, R., Arghavani, J., and Sohrabpour, S., 2012, "A Constitutive Model for Shape Memory Polymers With Application to Torsion of Prismatic Bars," J. Intel. Mat. Syst. Str., **23**(2), pp. 107–116.

[65] Baghani, M., Naghdabadi, R., and Arghavani, J., 2013, "A Large Eformation Framework for Shape Memory Polymers: Constitutive Modeling and Finite Element Implementation," J. Intel. Mat. Syst. Str., **24**(1), pp. 21–32.

[66] Yang, Q., and Li, G., 2016, "Temperature and Rate Dependent Thermomechanical Modeling of Shape Memory Polymers With Physics Based Phase Evolution Law," Int. J. Plast., **80**, pp. 168–186.

[67] Ge, Q., Serjouei, A., and Qi, H. J., 2016, "Thermomechanics of Printed Anisotropic Shape Memory Elastomeric Composites," Int. J. Solids Struct., **102**, pp. 186–199.

[68] Li, Y. X., Hu, J. Y., and Liu, Z. S., 2017, "A Constitutive Model of Shape Memory Polymers Based on Glass Transition and the Concept of Frozen Strain Release Rate," Int. J. Solids Struct., **124**, pp. 252–263.

[69] Lu, H. B., Wang, X. D., Yao, Y. T., and Fu, Y. Q., 2018, "A 'Frozen Volume' Transition Model and Working Mechanism for the Shape Memory Effect in Amorphous Polymers," Smart Mater. Struct., **27**(6), p. 065023.

[70] Arvanitakis, A. I., 2019, "A Constitutive Level-Set Model for Shape Memory Polymers and Shape Memory Polymeric Composites," Arch. Appl. Mech., **89**(9), pp. 1939–1951.

[71] Kim, J. H., Kang, T. J., and Yu, W. R., 2010, "Thermo-Mechanical Constitutive Modeling of Shape Memory Polyurethanes Using a Phenomenological Approach," Int. J. Plast., **26**(2), pp. 204–218.

[72] Gu, J., Sun, H., and Fang, C., 2015, "A Phenomenological Constitutive Model for Shape Memory Polyurethanes," J. Intel. Mat. Syst. Str., **26**(5), pp. 517–526.

[73] Wang, Z. D., Li, D. F., Xiong, Z. Y., and Chang, R. N., 2009, "Modeling Thermomechanical Behaviors of Shape Memory Polymer," J. Appl. Polym. Sci., **113**(1), pp. 651–656.

[74] Reese, S., Bo,´L. M., and Christ, D., 2010, "Finite Element-Based Multi-Phase Modelling of Shape Memory Polymer Stents," Comput. Method. Appl. Mech. Eng., **199**(21–22), pp. 1276–1286.

[75] Guo, X., Liu, L., Liu, Y., Zhou, B., and Leng, J., 2014, "Constitutive Model for a Stress-and Thermal-Induced Phase Transition in a Shape Memory Polymer," Smart Mater. Struct., **23**(10), p. 105019.

[76] Guo, X. G., Liu, L. W., Zhou, B., Liu, Y. J., and Leng, J. S., 2015, "Influence of Strain Rates on the Mechanical Behaviors of Shape Memory Polymer," Smart Mater. Struct., **24**(9), p. 095009.

[77] Guo, X., Liu, L., Zhou, B., Liu, Y. J., and Leng, J. S., 2016, "Constitutive Model for Shape Memory Polymer Based on the Viscoelasticity and Phase Transition Theories," J. Intel. Mat. Syst. Str., **27**(3), pp. 314–323.

[78] Scalet, G., Auricchio, F., Bonetti, E., Castellani, L., Ferri, D., Pachera, M., and Scavello, F., 2015, "An Experimental, Theoretical and Numerical Investigation of Shape Memory Polymers," Int. J. Plast., **67**, pp. 127–147.

[79] Park, H., Harrison, P., Guo, Z. Y., Lee, M. G., and Yu, W. R., 2016, "Three-Dimensional Constitutive Model for Shape Memory Polymers Using Multiplicative Decomposition of the Deformation Gradient and Shape Memory Strains," Mech. Mater., **93**, pp. 43–62.

[80] Bouaziz, R., Roger, F., and Prashantha, K., 2017, "Thermomechanical Modeling of Semi-Crystalline Thermoplastic Shape Memory Polymer Under Large Strain," Smart Mater. Struct., **26**(5), p. 055009.

[81] Guo, J. M., Liu, J., B., A., Wang, Z. Q., He, X. F., Hu, L. F., Tong, L. Y., and Tang, X. J., 2017, "A Thermodynamics Viscoelastic Constitutive Model for Shape Memory Polymers," J. Alloy. Compd., **705**, pp. 146–155.

[82] Li, Y. X., He, Y. H., and Liu, Z. S., 2017, "A Viscoelastic Constitutive Model for Shape Memory Polymers Based on Multiplicative Decompositions of the Deformation Gradient," Int. J. Plast., **91**, pp. 300–317.

[83] Zhao, W., Liu, L. W., Leng, J. S., and Liu, Y. J., 2020, "Thermo-Mechanical Behavior Prediction of Shape Memory Polymers Based on Multiplicative Decompositions of the Deformation Gradient," Mech. Mater., **143**, p. 103263.

[84] Pan'kov, A. A., 1999, "A Self-Consistent Statistical Mechanics Approach for Determining Effective Elastic Properties of Composites," Theor. Appl. Fract. Mech., **31**(3), pp. 157–161.

[85] Huang, Y., Hu, K. X., Wei, X., and Chandra, A., 1994, "A Generalized Self-Consistent Mechanics Method for Compositematerials With Multiphase Inclusions," J. Mech. Phys. Solids, **42**(3), pp. 491–504.

[86] Huang, Y., Hu, K. X., and Chandra, A., 1994, "A Self-Consistent Mechanics Method for Solids Containing Inclusions and a General Distribution of Cracks," Acta. Mech., **105**(1–4), pp. 69–84.

[87] Huang, Y., Hu, K. X., and Chandra, A., 1994, "A Generalized Self-Consistent Mechanics Method for Microcracked Solids," J. Mech. Phys. Solids, **42**(8), pp. 1273–1291.

[88] Huang, Y., and Hu, K. X., 1995, "A Generalized Self-Consistent Mechanics Method for Solids Containing Elliptical Inclusions," ASME J. Appl. Mech. Trans. ASME, **62**(3), pp. 566–572.

[89] Mori, T., and Tanaka, K., 1973, "Average Stress in Matrix and Average Elastic Energy of Materials With Misfitting Inclusions," Acta Metall., **1973**, 21(5), pp. 571–574.

[90] Yang, Q. S., He, X. Q., Liu, X., Leng, F. F., and Mai, Y. W., 2012, "The Effective Properties and Local Aggregation Effect of CNT/SMP Composites," Compos. Part B Eng., **43**(1), pp. 33–38.

[91] Xu, W., and Li, G. Q., 2010, "Constitutive Modeling of Shape Memory Polymer Based Self-Healing Syntactic Foam," Int. J. Solids Struct., **47**(9), pp. 1306–1316.

[92] Xu, W., and Li, G. Q., 2011, "Thermoviscoplastic Modeling and Testing of Shape Memory Polymer Based Self-Healing Syntactic Foam Programmed at Glassy Temperature," ASME J. Appl. Mech., **78**(6), p. 061017.

[93] Baghani, M., Naghdabadi, R., Arghavani, J., and Sohrabpour, S., 2012, "A Thermodynamically-Consistent 3D Constitutive Model for Shape Memory Polymers," Int. J. Plast., **35**, pp. 13–30.

[94] Abishera, R., Velmurugan, R., and Gopal, K. V. N., 2017, "Reversible Plasticity Shape Memory Effect in Epoxy/CNT Nanocomposites-A Theoretical Study," Compos. Sci. Technol., **141**, pp. 145–153.

[95] Jarali, C. S., Madhusudan, M., Vidyashankar, S., and Raja, S., 2018, "A New Micromechanics Approach to the Application of Eshelby's Equivalent Inclusion Method in Three Phase Composites With Shape Memory Polymer Matrix," Compos. Part B-Eng, **152**, pp. 17–30.

[96] Taherzadeh, M., Baghani, M., Baniassadi, M., Abrinia, K., and Safdari, M., 2016, "Modeling and Homogenization of Shape Memory Polymer Nanocomposites," Compos. Part B-Eng., **91**, pp. 36–43.

[97] Yin, C. X., Zeng, H., Gu, J. P., Xie, Z. M., and Sun, H. Y., 2019, "Modeling the Thermomechanical Behaviors of Particle Reinforced Shape Memory Polymer Composites," Appl. Phys. A-Mater., **125**(6), p. 382.

[98] Zeng, H., Leng, J., Gu, J., and Sun, H. Y., 2019, "Modeling the Thermomechanical Behaviors of Shape Memory Polymers and Their Nanocomposites by a Network Transition Theory," Smart Mater. Struct., **28**(6), p. 065018.

[99] Yarali, E., Baniassadi, M., and Baghani, M., 2019, "Numerical Homogenization of Coiled Carbon Nanotube Reinforced Shape Memory Polymer Nanocomposites," Smart Mater. Struct., **28**(3), p. 035026.

[100] Zeng, H., Pan, N., Gu, J., and Sun, H. Y., 2020, "Modeling the Thermoviscoelasticity of Transversely Isotropic Shape Memory Polymer Composites," Smart Mater. Struct., **29**(2), p. 025012.

[101] Zhao, W., Liu, L., Leng, J., and Liu, Y. J., 2019, "Thermo-Mechanical Behavior Prediction of Particulate Reinforced Shape Memory Polymer Composite," Compos. Part B-Eng., 179, p. 107455.

[102] Nishikawa, M., Wakatsuki, K., and Takeda, N., 2010, "Thermomechanical Experiment and Analysis on Shape Recovery Properties of Shape Memory Polymer Influenced by Fiber Reinforcement," J. Mater. Sci., 45(14), pp. 3957–3960.

[103] Nishikawa, M., Wakatsuki, K., Yoshimura, A., and Takeda, N., 2012, "Effect of Fiber Arrangement on Shape Fixity and Shape Recovery in Thermally Activated Shape Memory Polymer-Based Composites," Compos. Part A-Appl. Sci. Manuf., 43(1), pp. 165–173.

[104] Ge, Q., Luo, X., Rodriguez, E. D., Zhang, X., Mather, P. T., Dunn, M. L., and Qi, H. J., 2012, "Thermomechanical Behavior of Shape Memory Elastomeric Composites," J. Mech. Phys. Solids, 60(1), pp. 67–83.

[105] Tan, Q., Liu, L. W., Liu, Y. J., and Leng, J. S., 2014, "Thermal Mechanical Constitutive Model of Fiber Reinforced Shape Memory Polymer Composite: Based on Bridging Model," Compos. Part A-Appl. Sci. Manf., 64, pp. 132–138.

[106] Roh, J. H., Kim, H. I., and Lee, S. Y., 2015, "Viscoelastic Effect on Unfolding Behaviors of Shape Memory Composite Booms," Compos. Struct., 133, pp. 235–245.

[107] Su, X., and Peng, X., 2019, "A Lamination Model for Shape Memory Polymer/Woven Fabric Composites," Int. J. Comput. Mat. Sci., 08(2), p. 1950004.

[108] Su, X., Wang, Y., and Peng, X., 2020, "An Anisotropic Visco-Hyperelastic Model for Thermally-Actuated Shape Memory Polymer-Based Woven Fabric-Reinforced Composites," Int. J. Plast., 129, p. 102697.

[109] Zeng, H., Leng, J. S., Gu, J. P., and Sun, H. Y., 2020, "Modeling the Thermomechanical Behaviors of Short Fiber Reinforced Shape Memory Polymer Composites," Int. J. Mech. Sci., 166, p. 105212.

[110] Gu, J. P., Leng, J. S., Sun, H. Y., Zeng, H., and Cai, Z. B., 2019, "Thermomechanical Constitutive Modeling of Fiber Reinforced Shape Memory Polymer Composites Based on Thermodynamics With Internal State Variables," Mech. Mater., 130, pp. 9–19.

[111] Guo, Z. Y., Peng, X. Q., and Moran, B., 2007, "Mechanical Response of Neo-Hookean Fiber Reinforced Incompressible Nonlinearly Elastic Solids," J. Solids Struct., 44(6), pp. 1949–1969.

[112] Peng, X. Q., Guo, Z. Y., Du, T. L., and Yu, W. R., 2013, "A Simple Anisotropic Hyperelastic Constitutive Model for Textile Fabrics With Application to Forming Simulation," Compos. Part B-Eng., 52, pp. 275–281.

[113] Hong, S. B., Jang, J. H., Park, H., Kim, J. G., Goo, N. S., and Yu, W. R., 2019, "Three-Dimensional Constitutive Model of Woven Fabric-Reinforced Shape Memory Polymer Composites Considering Thermal Residual Stress," Smart Mater. Struct., 28(3), p. 035023.

[114] Agoras, M., Lopez-Pamies, O., and Ponte Castañeda, P., 2009, "A General Hyperelastic Model for Incompressible Fiber-Reinforced Elastomers," J. Mech. Phys. Solids., 57(2), pp. 268–286.

[115] Lopez-Pamies, O., and Idiart, M. I., 2010, "Fiber-Reinforced Hyperelastic Solids: A Realizable Homogenization Constitutive Theory," J. Eng. Math., 68(1), pp. 57–83.

[116] Jimenez, F. L., 2016, "On the Isotropy of Randomly Generated Representative Volume Elements for Fiber-Reinforced Elastomers," Compos. Part B-Eng., 87, pp. 33–39.

[117] Michailidis, P. A., Triantafyllidis, N., Shaw, J. A., and Grummon, D. S., 2009, "Superelasticity and Stability of a Shape Memory Alloy Hexagonal Honeycomb Under in-Plane Compression," Int. J. Solids. Struct., 46(13), pp. 2724–2738.

[118] Michel, J. C., Lopez-Pamies, O., Ponte Castañeda, P., and Triantafyllidis, N., 2010, "Microscopic and Macroscopic Instabilities in Finitely Strained Fiber-Reinforced Elastomers," J. Mech. Phys. Solids, 58(11), pp. 1776–1803.

[119] Heinrich, C., Aldridge, M., Wineman, A. S., Kieffer, J., Waas, A. M., and Shahwan, K., 2012, "The Influence of the Representative Volume Element (RVE) Size on the Homogenized Response of Cured Fiber Composites," Model. Simul. Mater. Sci. Eng., 20(7), p. 075007.

[120] Lan, X., Liu, L. W., Liu, Y. J., Leng, J. S., and Du, S. Y., 2014, "Post Microbuckling Mechanics of Fibre-Reinforced Shape-Memory Polymers Undergoing Flexure Deformation," Mech. Mater., 72, pp. 46–60.

[121] Timoshenko, S. P., and Gere, J. M., 1962, Theory of Elastic Stability, 2nd ed., Dover Publications, New York.

[122] Rosen, B. W., 1965, Fiber Composite Materials, American Metal Institute of Ohio, OH, pp. 123–187.

[123] Gall, K., Mikulas, M., Munshi, N. A., Beavers, F., and Tupper, M., 2000, "Carbon Fiber Reinforced Shape Memory Polymer Composites," J. Intel. Mat. Syst. Str., 11(11), pp. 877–886.

[124] Ware, T., Ellson, G., Kwasnik, A., Drewicz, S., Gall, K., and Voit, W., 2011, "Tough Shape Memory Polymer—Fiber Composites," J. Reinf. Plast. Comp., 30(5), pp. 371–380.

[125] Schultz, M. R., Francis, W. H., Campbell, D., and Lake, M. S., 2007, "Analysis Techniques for Shape-Memory Composite Structures," AIAA Paper No. 2007–2401.

[126] Campbell, D., and Lake, M. S., 2005, "Elastic Memory Composite Material: An Enabling Technology for Future Furlable Space Structures," AIAA Paper No. 2005–2362.

[127] Francis, W., Lake, M., Schultz, M., Campbell, D., Dunn, M., and Qi, H. J., 2007, "Elastic Memory Composite Microbuckling Mechanics: Closed-Form Model With Empirical Correlation," AIAA Paper No. 2007–2164.

[128] Campbell, D., and Maji, A. K., 2006, "Failure Mechanisms and Deployment Accuracy of Elastic Memory Composites," J. Aerosp. Eng., 19(3), pp. 184–193.

[129] Campbell, D., 2003, "Deployment Precision and Mechanics of Elastic Memory Composites," AIAA Paper No. 2003–1495.

[130] Chen, X., and Hutchinson, J. W., 2004, "Herringbone Buckling Patterns of Compressed Thin Films on Compliant Substrates," ASME J. Appl. Mech., 71(5), pp. 597–603.

[131] Huang, Z. Y., Hong, W., and Suo, Z., 2005, "Nonlinear Analyses of Wrinkles in a Film Bonded to a Compliant Substrate," J. Mech. Phys. Solids, 53(9), pp. 2101–2118.

[132] Xiao, J., Ryu, S. Y., Huang, Y., Hwang, K. C., Paik, U., and Rogers, J. A., 2010, "Mechanics of Nanowire/Nanotube in-Surface Buckling on Elastomeric Substrates," Nanotechnology, 21(8), p. 085708.

[133] Ryu, S. Y., Xiao, J. L., Park, W. I., Son, K. S., Huang, Y. G., Paik, U., and Rogers, J. A., 2009, "Lateral Buckling Mechanics in Silicon Nanowires on Elastomeric Substrates," Nano Lett., 9(9), pp. 3214–3219.

[134] Campbell, D., Lake, M., and Mallick, K., 2004, "A Study of the Bending Mechanics of Elastic Memory Composites," AIAA Paper No. 2004–1636.

[135] Jeon, H. G., Mather, P. T., and Haddad, T. S., 2000, "Shape Memory and Nanostructure in Poly (Norbornyl-POSS) Copolymers," Polym. Int., 49(5), pp. 453–457.

[136] Lake, M., Hazelton, C., Murphey, T., and Murphy, D., 2002, "Development of Coilable Longerons Using Elastic Memory Composite Material," AIAA Paper No. 2002–1453.

[137] Wang, Z. D., Li, Z. F., Xiong, Z. Y., and Wang, L. Y., 2010, "Theoretical Studies on Microbuckling Mode of Elastic Memory Composites," Acta Mech. Solida Sin., 23(1), pp. 20–28.

[138] Wang, Z. D., Xiong, Z. Y., Li, Z. F., and Chang, R. N., 2008, "Micromechanism of Deformation in EMC Laminates," Mat. Sci. Eng. A-Struct., 496(1–2), pp. 323–328.

[139] Tan, Q., Liu, L. W., Liu, Y. J., and Leng, J. S., 2013, "Post Buckling Analysis of the Shape Memory Polymer Composite Laminate Bonded With Alloy Film," Compos. Part B-Eng., 53, pp. 218–225.

[140] Zhang, J., Dui, G., and Liang, X., 2018, "Revisiting the Micro-Buckling of Carbon Fibers in Elastic Memory Composite Plates Under Pure Bending," Int. J. Mech. Sci., 136, pp. 339–348.